

Studies on numerical verification for the bifurcation phenomena  
of the Hénon equation

エノン方程式の分岐に対する精度保証付き数値計算の研究

February, 2023

Taisei ASAI  
浅井 大晴

Studies on numerical verification for the bifurcation phenomena  
of the Hénon equation

エノン方程式の分岐に対する精度保証付き数値計算の研究

February, 2023

Waseda University Graduate School of Fundamental Science and  
Engineering

Department of Pure and Applied Mathematics, Research on Numerical  
Analysis

Taisei ASAI  
浅井 大晴

# Contents

Chapter 1	Overview	2
Chapter 2	Basic numerical verification method and newly discovered solutions of the Hénon equation	3
2.1	Introduction . . . . .	3
2.2	Preliminaries . . . . .	4
2.3	Numerical verification method . . . . .	6
2.4	Evaluation for $\alpha$ and $\beta$ . . . . .	7
2.5	Numerical results . . . . .	11
2.6	Short summary of chapter 2 . . . . .	18
Chapter 3	Advanced numerical verification method and analysis of bifurcation phenomena of the Hénon equation	19
3.1	Introduction . . . . .	19
3.2	Preliminaries . . . . .	20
3.3	Numerical verification method . . . . .	21
3.4	Evaluation for $\alpha$ and $\beta$ . . . . .	22
3.5	Consideration of singularity . . . . .	26
3.6	Numerical results of the existence of solutions . . . . .	28
3.7	Branches . . . . .	31
3.8	Numerical results of bifurcation branches . . . . .	34
3.9	Bifurcation point . . . . .	35
3.10	Numerical results of the bifurcation point . . . . .	38
3.11	Short summary of chapter 3 . . . . .	39
Chapter 4	Conclusion	40
	Acknowledgments	41
	References	42

# Chapter 1

## Overview

In this paper, we consider the Hénon equation

$$\begin{cases} -\Delta u = |\mathbf{x} - \mathbf{x}_0|^l |u|^{p-1} u & \text{in } \Omega, \\ u = 0 & \text{on } \partial\Omega, \end{cases}$$

where  $\Omega \subset \mathbb{R}^N$  ( $N = 1, 2, 3$ ) is a bounded domain. The real parameter  $l \geq 0$  is the potential index, and the real parameter  $2 \leq p < p^*$  ( $p^* = \infty$  if  $N = 1, 2$  and  $p^* = 5$  if  $N = 3$ ) is the polytropic index. This Hénon equation, a generalized form of the Emden equation, admits symmetry-breaking bifurcation for the potential index  $l$ . Therefore, it has asymmetric solutions on a symmetric domain even though the Emden equation has no asymmetric unidirectional solution on such a domain. In chapter 2, we discuss a numerical verification method for proving the existence of solutions of the Hénon equation on a bounded domain. By applying the method to a line-segment domain and a square domain, we numerically prove the existence of several solutions of the Hénon equation for  $l = 0, 2, 4$  with fixed  $p = 3$ . As a result, we find a set of undiscovered solutions with three peaks on the square domain.

However, the singularity of the Hénon equation prevents to verify the solution when the parameter  $l$  is not even number using only the chapter 2 method. It also makes it difficult to verify the bifurcation point and branches. In chapter 3, we focused on the one-dimensional Hénon equation

$$\begin{cases} -u'' = |x|^l |u|^{p-1} u, & x \in (-1, 1), \\ u(-1) = u(1) = 0, \end{cases}$$

and developed a numerical verification method that follows the singularity of the Hénon equation. By applying the method, the existence of multiple solutions can be proved efficiently even when  $l$  is not even number. As a result, we succeeded in verifying the branches and bifurcation points of the simple symmetry-breaking bifurcation of the one-dimensional Hénon equation.

## Chapter 2

# Basic numerical verification method and newly discovered solutions of the Hénon equation

### 2.1 Introduction

The Hénon equation was proposed as a model for mass distribution in spherically symmetric star clusters, which is important in studying the stability of rotating stars [1]. One important aspect of the model is the Dirichlet boundary value problem

$$\begin{cases} -\Delta u = |\mathbf{x} - \mathbf{x}_0|^l |u|^{p-1} u & \text{in } \Omega, \\ u = 0 & \text{on } \partial\Omega, \end{cases} \quad (2.1)$$

where  $\Omega \subset \mathbb{R}^N$  ( $N = 1, 2, 3$ ) is a bounded domain,  $\mathbf{x}$  is the location of the star, and  $u$  is the positive solution because it stands for the stellar density. Particularly,  $\mathbf{x}_0$  is often set to the center of the symmetry axis if the domain has some symmetry. The real parameter  $2 \leq p < p^*$  ( $p^* = \infty$  if  $N = 1, 2$  and  $p^* = 5$  if  $N = 3$ ) is the polytropic index, determined according to the central density of each stellar type. The real parameter  $l \geq 0$  is the ratio of the transverse velocity to the radial velocity. These velocities can be derived by decomposing the space velocity vector into the radial and transverse components.

When  $l = 0$ , the Hénon equation coincides with the Emden equation  $-\Delta u = |u|^{p-1} u$  in  $\Omega$ . In this case, the transverse velocity vanishes and the orbit becomes purely radial. Gidas, Ni, and Nirenberg proved that the Emden equation has no asymmetric unidirectional solution in a rectangle domain [2]. However, Breuer, Plum, and McKenna reported some asymmetric solutions obtained with an approximate computation based on the Galerkin method [3], which were called “spurious approximate solutions” caused by discretization errors. This example shows the need to verify approximate computations. By contrast, a theoretical analysis [4] for large  $l$  (when the orbit tends to be purely circular) found that the Hénon equation admits symmetry-breaking bifurcation, thereby having several asymmetric solutions even on a symmetric domain.

The importance of the Hénon equation has led to active mathematical study on it over the last decade. For example, Amadori and Gladiali [5] analyzed the bifurcation

structure of (2.1) with respect to parameter  $p$ . They applied an analytical method to the Hénon equation that had worked for the Emden equation. Additionally, several numerical studies have been conducted on the Hénon equation [6, 7, 8, 9]. In particular, we are motivated by the work of Yang, Li, and Zhu [6], who developed an effective computational method to find multiple asymmetric solutions of (2.1) on the unit square  $\Omega = (0, 1)^2$  using algorithms based on the bifurcation method. They generated the bifurcation curve of (2.1) with  $p = 3$  and numerically predicted bifurcation points around  $l = 0.5886933$  and  $l = 2.3654862$  using approximate computations.

The purpose of our study is to prove the existence of solutions of (2.1) using the Newton–Kantorovich theorem (see Theorem 2). We prove their existence through the following steps:

1. We construct approximate solutions  $\hat{u}$  using the Galerkin method with polynomial approximations.
2. Using the Newton–Kantorovich theorem (Theorem 3), we prove the existence of solutions  $u$  of (2.1) with nearby approximations  $\hat{u}$  while sharply evaluating the error bound between  $u$  and  $\hat{u}$  in terms of the  $H_0^1$ -norm  $\|\nabla \cdot\|_{L^2}$ .

By applying the above steps to the problem (2.1) on the domains  $\Omega = (0, 1)^N$  ( $N = 1, 2$ ), we successfully prove the existence of several solutions for  $l = 0, 2, 4$ . In particular, we find a set of solutions with three peaks, which were not revealed in [6] (see Figure 2.2).

The remainder of this chapter is organized as follows. Some notation is introduced in Section 2.2. Sections 2.3 and 2.4 describe numerical verification based on the Newton–Kantorovich theorem together with evaluations of several required constants. Section 2.5 shows the results numerically proving the existence of several asymmetric solutions of (2.1). Subsequently, we discuss the solution curves of the problem for  $p = 3$  based on an approximate computation.

## 2.2 Preliminaries

We begin by introducing some notation. For two Banach spaces  $X$  and  $Y$ , the set of bounded linear operators from  $X$  to  $Y$  is denoted by  $\mathcal{L}(X, Y)$ . The norm of  $T \in \mathcal{L}(X, Y)$  is defined by

$$\|T\|_{\mathcal{L}(X, Y)} := \sup_{0 \neq u \in X} \frac{\|Tu\|_Y}{\|u\|_X}. \quad (2.2)$$

Let  $L^p(\Omega)$  ( $1 \leq p < \infty$ ) be the function space of  $p$ -th power Lebesgue integrable functions over a domain  $\Omega$  with the  $L^p$ -norm  $\|u\|_{L^p} := (\int_{\Omega} |u(x)|^p dx)^{1/p} < \infty$ . When  $p = 2$ ,  $L^2(\Omega)$  is the Hilbert space with the inner product  $(u, v)_{L^2} := \int_{\Omega} u(x)v(x)dx$ . Let  $L^\infty(\Omega)$  be the function space of Lebesgue measurable functions over  $\Omega$ , with the norm  $\|u\|_{L^\infty} := \text{ess sup}\{|u(x)| : x \in \Omega\}$  for  $u \in L^\infty(\Omega)$ . We denote the first-order  $L^2$  Sobolev space in  $\Omega$  as  $H^1(\Omega)$  and define

$$H_0^1(\Omega) := \{u \in H^1(\Omega) : u = 0 \text{ on } \partial\Omega \text{ in the trace sense}\}$$

as the solution space for the target equation (2.1). We endow  $H_0^1(\Omega)$  with the inner product and norm

$$(u, v)_{H_0^1} := (\nabla u, \nabla v)_{L^2} + \tau(u, v)_{L^2}, \quad u, v \in H_0^1(\Omega), \quad (2.3)$$

$$\|u\|_{H_0^1} := \sqrt{(u, u)_{H_0^1}}, \quad u \in H_0^1(\Omega), \quad (2.4)$$

where  $\tau$  is a nonnegative number chosen as

$$\tau > -p|\mathbf{x} - \mathbf{x}_0|^l |\hat{u}(\mathbf{x})|^{p-1} \quad \text{a.e. } \mathbf{x} \in \Omega \quad (2.5)$$

for a numerically computed approximation  $\hat{u} \in H_0^1(\Omega)$ . The condition (2.5) is required in Subsection 2.4.2 and  $\hat{u}$  is explicitly constructed in Section 2.5. Because the norm  $\|\cdot\|_{H_0^1}$  monotonically increases with respect to  $\tau$ , the  $H_0^1(\Omega)$  norm  $\|\nabla \cdot\|_{L^2}$  is dominated by the norm  $\|\cdot\|_{H_0^1}$  for all  $\tau \geq 0$ . Therefore, the error bound  $\|u - \hat{u}\|_{H_0^1}$  is always an upper bound for  $\|\nabla(u - \hat{u})\|_{L^2}$ . The topological dual space of  $H_0^1(\Omega)$  is denoted by  $H^{-1}$  with the norm defined by

$$\|T\|_{H^{-1}} := \sup_{0 \neq u \in H_0^1} \frac{|Tu|}{\|u\|_{H_0^1}}.$$

The bound for the embedding  $H_0^1(\Omega) \hookrightarrow L^p(\Omega)$  is denoted by  $C_p$  ( $p \geq 2$ ). More precisely,  $C_p$  is a positive number satisfying

$$\|u\|_{L^p} \leq C_p \|u\|_{H_0^1} \quad \text{for all } u \in H_0^1(\Omega). \quad (2.6)$$

Note that  $\|u\|_{H^{-1}} \leq C_p \|u\|_{L^{p'}}$ ,  $u \in L^{p'}(\Omega)$  holds for  $p'$  satisfying  $p^{-1} + p'^{-1} = 1$ . Explicitly estimating the embedding constant  $C_p$  is important for our numerical verification. When  $p = 2$ , we use the following optimal inequality:

$$\|u\|_{L^2} \leq \frac{1}{\sqrt{\lambda_1 + \tau}} \|u\|_{H_0^1},$$

where  $\lambda_1$  is the first eigenvalue of the minus Laplacian in the weak sense. Especially when  $\Omega = (0, 1)^N$ , we have  $\lambda_1 = N\pi^2$ . When  $p$  is not 2, we use the following theorems depending on the dimension of  $\Omega$ . We use [10, Lemma 7.12] to obtain an explicit value of  $C_p$  for a one-dimensional bounded domain.

**Theorem 1** ( [10, Lemma 7.12] ) *Let  $\Omega = (a, b) \subset \mathbb{R}$ , with  $a \in \mathbb{R} \cup \{-\infty\}$ ,  $b \in \mathbb{R} \cup \{+\infty\}$ ,  $a < b$ . Moreover, let  $\rho^*$  denote the minimal point of the spectrum of  $-u''$  on  $H_0^1(\Omega)$ , i.e.  $\rho^* = \pi^2/(b-a)^2$  if  $(a, b)$  is bounded. Then, for all  $u \in H_0^1(\Omega)$ ,*

$$\|u\|_{L^p} \leq C_p \|u\|_{H_0^1} \quad (p \in (2, \infty)),$$

where, abbreviating  $\varepsilon := \frac{2}{p} \in (0, 1)$ ,

$$C_p := \begin{cases} \frac{1}{\sqrt{2}}(1-\varepsilon)^{\frac{1}{4}(1-\varepsilon)}(1+\varepsilon)^{\frac{1}{4}(1+\varepsilon)}\tau^{-\frac{1}{4}(1+\varepsilon)} & \text{if } \rho^* \leq \tau \frac{1-\varepsilon}{1+\varepsilon}, \\ \frac{1}{\sqrt{\rho^* + \tau}}(\rho^*)^{\frac{1}{4}(1-\varepsilon)} & \text{otherwise,} \end{cases}$$

for  $p \in (2, \infty)$ .

When  $N \geq 2$ , we use [11, Corollary A.2] or [10, Lemma 7.10] to obtain  $C_p$  for bounded domains  $\Omega \subset \mathbb{R}^N$ . In our numerical experiments in Section 2.5,  $C_p$  evaluated by [11, Corollary A.2] is smaller than that evaluated by [10, Lemma 7.10]. In [11, Corollary A.2],  $C_p$  is evaluated for  $\|u\|_{L^p} \leq C_p \|\nabla u\|_{L^2}$ , but since  $\|\nabla u\|_{L^2} \leq \|u\|_{H_0^1}$  for all  $\tau$ , the same  $C_p$  can be used for  $\|u\|_{L^p} \leq C_p \|u\|_{H_0^1}$ .

**Theorem 2** ([11, Corollary A.2]) *Let  $\Omega \subset \mathbb{R}^N (N \geq 2)$  be a bounded domain, the measure of which is denoted by  $|\Omega|$ . Let  $p \in (N/(N-1), 2N/(N-2)]$  if  $N \geq 3$ ,  $p \in (2, \infty)$  if  $N = 2$ . We set  $q = Np/(N+p)$ . Then, (2.6) holds for*

$$C_p(\Omega) = |\Omega|^{\frac{2-q}{2q}} T_p.$$

Here,  $T_p$  is defined by

$$T_p = \pi^{-\frac{1}{2}} N^{-\frac{1}{q}} \left( \frac{q-1}{N-q} \right)^{1-\frac{1}{q}} \left\{ \frac{\Gamma(1+\frac{N}{2}) \Gamma(N)}{\Gamma(\frac{N}{q}) \Gamma(1+N-\frac{N}{q})} \right\}^{\frac{1}{N}},$$

where  $\Gamma$  is the gamma function.

### 2.3 Numerical verification method

This section discusses the numerical verification method used in this chapter. We first define the operator  $f$  as

$$f : \begin{cases} u(\cdot) & \mapsto |\cdot - \mathbf{x}_0|^l |u(\cdot)|^{p-1} u(\cdot), \\ H_0^1(\Omega) & \rightarrow H^{-1}, \end{cases}$$

where  $2 \leq p < p^*$  ( $p^* = \infty$  if  $N = 1, 2$  and  $p^* = 5$  if  $N = 3$ ). Furthermore, we define the nonlinear operator  $F : H_0^1(\Omega) \rightarrow H^{-1}$  by  $F(u) := -\Delta u - f(u)$ , which is given by

$$\langle F(u), v \rangle = (\nabla u, \nabla v)_{L^2} - \langle f(u), v \rangle \quad \text{for all } v \in H_0^1(\Omega),$$

where  $\langle f(u), v \rangle = \int_{\Omega} (|\mathbf{x} - \mathbf{x}_0|^l |u(\mathbf{x})|^{p-1} u(\mathbf{x})) v(\mathbf{x}) d\mathbf{x}$ . The Fréchet derivatives of  $f$  and  $F$  at  $\varphi \in H_0^1(\Omega)$  are denoted by  $f'_{\varphi}$  and  $F'_{\varphi}$ , respectively, and given by

$$\langle f'_{\varphi} u, v \rangle = \int_{\Omega} (p |\mathbf{x} - \mathbf{x}_0|^l |\varphi(\mathbf{x})|^{p-1} u(\mathbf{x})) v(\mathbf{x}) d\mathbf{x} \quad \text{for all } u, v \in H_0^1(\Omega), \quad (2.7)$$

$$\langle F'_{\varphi} u, v \rangle = (\nabla u, \nabla v)_{L^2} - \langle f'_{\varphi} u, v \rangle \quad \text{for all } u, v \in H_0^1(\Omega). \quad (2.8)$$

Then, we consider the following problem:

$$\text{Find } u \in H_0^1(\Omega) \quad \text{s.t.} \quad F(u) = 0, \quad (2.9)$$

which is the weak form of the problem (2.1). To conduct the numerical verification for this problem, we apply the Newton–Kantorovich theorem, which enables us to prove the existence of a true solution  $u$  near a numerically computed “good” approximate solution  $\hat{u}$  (see, for example, [12]). Hereafter,  $B(\hat{u}, r)$  and  $\bar{B}(\hat{u}, r)$  respectively denote the open and closed balls with center approximate solution  $\hat{u}$  and radius  $r$  in terms of norm  $\|\cdot\|_{H_0^1}$ .



**Theorem 3 (Newton–Kantorovich’s theorem)** *Let  $\hat{u} \in H_0^1(\Omega)$  be some approximate solution of  $F(u) = 0$ . Suppose that there exists some  $\alpha > 0$  satisfying*

$$\|F'_{\hat{u}}{}^{-1}F(\hat{u})\|_{H_0^1} \leq \alpha. \quad (2.10)$$

Moreover, suppose that there exists some  $\beta > 0$  satisfying

$$\|F'_{\hat{u}}{}^{-1}(F'_v - F'_w)\|_{\mathcal{L}(H_0^1, H_0^1)} \leq \beta \|v - w\|_{H_0^1}, \quad \text{for all } v, w \in D, \quad (2.11)$$

where  $D = B(\hat{u}, 2\alpha + \delta)$  is an open ball depending on the above value  $\alpha > 0$  for small  $\delta > 0$ . If

$$\alpha\beta \leq \frac{1}{2},$$

then there exists a solution  $u \in H_0^1(\Omega)$  of  $F(u) = 0$  in  $\bar{B}(\hat{u}, \rho)$  with

$$\rho = \frac{1 - \sqrt{1 - 2\alpha\beta}}{\beta}.$$

Furthermore, the solution  $u$  is unique in  $\bar{B}(\hat{u}, 2\alpha)$ .

## 2.4 Evaluation for $\alpha$ and $\beta$

To apply Theorem 3 to the numerical verification for problem (2.1), we need to explicitly evaluate  $\alpha$  and  $\beta$ . The left side of (2.10) is evaluated as

$$\|F'_{\hat{u}}{}^{-1}F(\hat{u})\|_{H_0^1} \leq \|F'_{\hat{u}}{}^{-1}\|_{\mathcal{L}(H^{-1}, H_0^1)} \|F(\hat{u})\|_{H^{-1}}.$$

Therefore, we set

$$\alpha = \|F'_{\hat{u}}{}^{-1}\|_{\mathcal{L}(H^{-1}, H_0^1)} \|F(\hat{u})\|_{H^{-1}}.$$

Moreover, the left side of (2.11) is estimated as

$$\begin{aligned} \|F'_{\hat{u}}{}^{-1}(F'_v - F'_w)\|_{\mathcal{L}(H_0^1, H_0^1)} &\leq \|F'_{\hat{u}}{}^{-1}\|_{\mathcal{L}(H^{-1}, H_0^1)} \|F'_v - F'_w\|_{\mathcal{L}(H_0^1, H^{-1})} \\ &= \|F'_{\hat{u}}{}^{-1}\|_{\mathcal{L}(H^{-1}, H_0^1)} \|f'_v - f'_w\|_{\mathcal{L}(H_0^1, H^{-1})}. \end{aligned}$$

Hence, the desired value of  $\beta$  is obtained via

$$\beta \leq \|F'_{\hat{u}}{}^{-1}\|_{\mathcal{L}(H^{-1}, H_0^1)} L,$$

where  $L$  is the Lipschitz constant satisfying

$$\|f'_v - f'_w\|_{\mathcal{L}(H_0^1, H^{-1})} \leq L \|v - w\|_{H_0^1} \quad \text{for all } v, w \in D. \quad (2.12)$$

We are left to evaluate the inverse operator norm  $\|F'_{\hat{u}}{}^{-1}\|_{\mathcal{L}(H^{-1}, H_0^1)}$ , the residual norm  $\|F(\hat{u})\|_{H^{-1}}$ , and the Lipschitz constant  $L$  for problem (2.9).

### 2.4.1 Residual norm $\|F(\hat{u})\|_{H^{-1}}$

If the approximation  $\hat{u}$  is sufficiently smooth so that  $\Delta\hat{u} \in L^2(\Omega)$ , we can evaluate the residual norm  $\|F(\hat{u})\|_{H^{-1}}$  as follows:

$$\|F(\hat{u})\|_{H^{-1}} \leq C_2 \|\Delta\hat{u} + f(\hat{u})\|_{L^2}, \quad (2.13)$$

where  $C_2$  is the embedding constant satisfying (2.6) for  $p = p' = 2$ . Our numerical experiments discussed in Section 2.5 use this evaluation, calculating the  $L^2$ -norm via stable numerical integration with all rounding errors strictly estimated.

However, the condition  $\Delta\hat{u} \in L^2(\Omega)$  is not satisfied such as when we construct  $\hat{u}$  with a piecewise linear finite element basis. We use the method of [10, Subsection 7.2] to evaluate the residual norm applicable to such a case. The following is a brief description of the evaluation method. First, we find an approximation  $\rho \in H(\operatorname{div}, \Omega) = \{\tau \in L^2(\Omega)^N : \operatorname{div} \tau \in L^2(\Omega)\}$  to  $\nabla\hat{u}$ . Then, the residual norm is evaluated as

$$\begin{aligned} \|F(\hat{u})\|_{H^{-1}} &= \|-\Delta\hat{u} - f(\hat{u})\|_{H^{-1}}, \\ &= \|-\Delta\hat{u} + \operatorname{div} \rho - \operatorname{div} \rho - f(\hat{u})\|_{H^{-1}}, \\ &\leq \|\operatorname{div}(-\nabla\hat{u} + \rho)\|_{H^{-1}} + \|\operatorname{div} \rho + f(\hat{u})\|_{H^{-1}}, \\ &\leq \|-\nabla\hat{u} + \rho\|_{L^2} + C_2 \|\operatorname{div} \rho + f(\hat{u})\|_{L^2}, \end{aligned}$$

where we used  $\|\operatorname{div} \omega\|_{H^{-1}} \leq \|\omega\|_{L^2}$  for  $\omega \in H(\operatorname{div}, \Omega)$ . As mentioned in [10, Subsection 7.2],  $\rho$  can be computed without additional computational resources when we use the mixed finite element method to construct  $\hat{u}$ .

### 2.4.2 Inverse operator norm $\|F'_{\hat{u}}\|_{\mathcal{L}(H^{-1}, H_0^1)}$

In this subsection, we evaluate the inverse operator norm  $\|F'_{\hat{u}}\|_{\mathcal{L}(H^{-1}, H_0^1)}$ . To this end, we use the following theorem.

**Theorem 4 ([13])** *Let  $\Phi : H_0^1(\Omega) \rightarrow H^{-1}$  be the canonical isometric isomorphism; that is,  $\Phi$  is given by*

$$\langle \Phi u, v \rangle := (u, v)_{H_0^1} \quad \text{for } u, v \in H_0^1(\Omega).$$

If

$$\mu_0 := \min \{ |\mu| : \mu \in \sigma_p(\Phi^{-1}F'_{\hat{u}}) \cup \{1\} \} \quad (2.14)$$

is positive, then the inverse of  $F'_{\hat{u}}$  exists, and we have

$$\|F'_{\hat{u}}\|_{\mathcal{L}(H^{-1}, H_0^1)} \leq \mu_0^{-1}, \quad (2.15)$$

where  $\sigma_p(\Phi^{-1}F'_{\hat{u}})$  denotes the point spectrum of  $\Phi^{-1}F'_{\hat{u}}$ .

The eigenvalue problem  $\Phi^{-1}F'_{\hat{u}}u = \mu u$  in  $H_0^1(\Omega)$  is equivalent to

$$(\nabla u, \nabla v)_{L^2} - \langle f'_{\hat{u}}u, v \rangle = \mu (u, v)_{H_0^1} \quad \text{for all } v \in H_0^1(\Omega), \quad (2.16)$$

where  $(u, v)_{H_0^1}$  denotes the inner product defined in (2.3) that depends on  $\tau$  and  $\langle f'_u u, v \rangle$  is given by (2.7).

We consider the operator  $\mathcal{N} := \Phi - F'_u$  from  $H_0^1(\Omega)$  to  $H^{-1}$ , which satisfies  $\langle \mathcal{N}u, v \rangle = \int_{\Omega} (p|\mathbf{x} - \mathbf{x}_0|^l |\hat{u}(\mathbf{x})|^{p-1}) u(\mathbf{x}) v(\mathbf{x}) d\mathbf{x}$  for all  $u, v \in H_0^1(\Omega)$ . Because  $\mathcal{N}$  maps  $H_0^1(\Omega)$  into  $L^2(\Omega)$  and the embedding  $L^2(\Omega) \hookrightarrow H^{-1}$  is compact,  $\mathcal{N} : H_0^1(\Omega) \rightarrow H^{-1}$  is a compact operator. Therefore,  $F'_u$  is a Fredholm operator, and the spectrum  $\sigma(\Phi^{-1}F'_u)$  of  $\Phi^{-1}F'_u$  is given by

$$\sigma(\Phi^{-1}F'_u) = 1 - \sigma(\Phi^{-1}\mathcal{N}) = 1 - \{\sigma_p(\Phi^{-1}\mathcal{N}) \cup \{0\}\} = \sigma_p(\Phi^{-1}F'_u) \cup \{1\}.$$

Accordingly, it suffices to look for eigenvalues  $\mu \neq 1$ . By setting  $\lambda = (1 - \mu)^{-1}$ , we further transform this eigenvalue problem into

$$\text{Find } u \in H_0^1(\Omega) \text{ and } \lambda \in \mathbb{R} \text{ s.t. } (u, v)_{H_0^1} = \lambda \langle (\tau + f'_u)u, v \rangle \text{ for all } v \in H_0^1(\Omega), \quad (2.17)$$

where  $\langle (\tau + f'_u)u, v \rangle = \int_{\Omega} (\tau + p|\mathbf{x} - \mathbf{x}_0|^l |\hat{u}(\mathbf{x})|^{p-1}) u(\mathbf{x}) v(\mathbf{x}) d\mathbf{x}$  for  $u, v \in H_0^1(\Omega)$ . Because  $\tau$  is chosen so that  $\tau + f'_u$  becomes positive (see (2.5)), (2.17) is a regular eigenvalue problem, the spectrum of which consists of a sequence  $\{\lambda_k\}_{k=1}^{\infty}$  of eigenvalues converging to  $+\infty$ . To compute  $\|F'_u\|_{\mathcal{L}(H^{-1}, H_0^1)}$  on the basis of Theorem 4, we need to enclose the eigenvalue  $\lambda$  of (2.17) that minimizes the corresponding absolute value of  $|\mu|$  ( $= |1 - \lambda^{-1}|$ ). We consider the approximate eigenvalue problem

$$\text{Find } u_M \in V_M \text{ and } \lambda^M \in \mathbb{R} \text{ s.t. } (u_M, v_M)_{H_0^1} = \lambda^M \langle (\tau + f'_u)u_M, v_M \rangle \text{ for all } v_M \in V_M, \quad (2.18)$$

where  $V_M$  is a finite-dimensional subspace of  $H_0^1(\Omega)$  such as the space spanned by the finite element basis and Fourier basis. For our problem,  $V_M$  will be explicitly chosen in Section 2.5. Note that (2.18) is a matrix problem with eigenvalues that can be enclosed with rigorous computation techniques (see, for example, [14, 15, 16]).

We then estimate the error between the  $k$ -th eigenvalue  $\lambda_k$  of (2.17) and the  $k$ -th eigenvalue  $\lambda_k^M$  of (2.18). We consider the weak formulation of the Poisson equation,

$$(u_g, v)_{H_0^1} = (g, v)_{L^2} \text{ for all } v \in H_0^1(\Omega) \quad (2.19)$$

given  $g \in L^2(\Omega)$ . This equation has a unique solution  $u_g \in H_0^1(\Omega)$  for each  $g \in L^2(\Omega)$  [17]. Let  $P_M^\tau : H_0^1(\Omega) \rightarrow V_M$  be the orthogonal projection defined by

$$(P_M^\tau u - u, v_M)_{H_0^1} = 0 \text{ for all } u \in H_0^1(\Omega) \text{ and } v_M \in V_M.$$

The following theorem enables us to estimate the error between  $\lambda_k$  and  $\lambda_k^M$ .

**Theorem 5** ([18, 19]) *Let  $\hat{u} \in H_0^1(\Omega) \cap L^\infty(\Omega)$ . Suppose that there exists  $C_M^\tau > 0$  such that*

$$\|u_g - P_M^\tau u_g\|_{H_0^1} \leq C_M^\tau \|g\|_{L^2} \quad (2.20)$$

for any  $g \in L^2(\Omega)$  and the corresponding solution  $u_g \in H_0^1(\Omega)$  of (2.19). Then,

$$\frac{\lambda_k^M}{\lambda_k^M (C_M^\tau)^2 \|\tau + f'_u\|_{L^\infty} + 1} \leq \lambda_k \leq \lambda_k^M,$$

where the  $L^\infty$ -norm is defined by  $\|\tau + f'_u\|_{L^\infty} := \text{esssup}\{|\tau + p|\mathbf{x} - \mathbf{x}_0|^l |\hat{u}(\mathbf{x})|^{p-1}| : \mathbf{x} \in \Omega\}$ .

The right inequality is known as the Rayleigh–Ritz bound, which is derived from the min-max principle:

$$\lambda_k = \min_{H_k \subset H_0^1(\Omega)} \left( \max_{v \in H_k \setminus \{0\}} \frac{\|v\|_{H_0^1}^2}{\|av\|_{L^2}^2} \right) \leq \lambda_k^M,$$

where  $a(\mathbf{x}) = \sqrt{\tau + p|\mathbf{x} - \mathbf{x}_0|^l |\hat{u}(\mathbf{x})|^{p-1}}$ , and the minimum is taken over all  $k$ -dimensional subspaces  $H_k$  of  $H_0^1(\Omega)$ . The left inequality was proved in [18, 19]. Assuming the  $H^2$ -regularity of solutions to (2.19) (which follows, for example, when  $\Omega$  is a convex polygonal domain [17, Section 3.3]), [18, Theorem 4] ensures the left inequality. A more general statement that does not require the  $H^2$ -regularity is proved in [19, Theorem 2.1].

When the solution of (2.19) has  $H^2$ -regularity, (2.20) can be replaced with

$$\|u - P_M^\tau u\|_{H_0^1} \leq C_M^\tau \|\Delta u + \tau u\|_{L^2} \quad \text{for all } u \in H^2(\Omega) \cap H_0^1(\Omega). \quad (2.21)$$

The constant  $C_M^\tau$  satisfying (2.21) is obtained as  $C_M^\tau = C_M \sqrt{1 + \tau(C_M)^2}$  (see [20, Remark A.4]), where we denote  $C_M = C_M^0$  with  $\tau = 0$ . For example, when  $\Omega = (0, 1)^N$ , an explicit value of  $C_M$  is obtained for  $V_M$  spanned by the Legendre polynomial basis using [21, Theorem 2.3]. This will be used for our computation in Section 2.5.

**Theorem 6 ([21])** *When  $\Omega = (0, 1)^N$ , the inequality*

$$\|\nabla(u - P_M u)\|_{L^2} \leq C_M \|\Delta u\|_{L^2} \quad \text{for all } u \in H^2(\Omega) \cap H_0^1(\Omega)$$

holds for

$$C_M = \max \left\{ \frac{1}{2(2M+1)(2M+5)} + \frac{1}{4(2M+5)\sqrt{2M+3}\sqrt{2M+7}}, \right. \\ \left. \frac{1}{4(2M+5)\sqrt{2M+3}\sqrt{2M+7}} + \frac{1}{2(2M+5)(2M+9)} + \frac{1}{4(2M+9)\sqrt{2M+7}\sqrt{2M+11}} \right\}^{\frac{1}{2}}.$$

### 2.4.3 Lipschitz constant $L$

Hereafter, we denote  $d(=d(\Omega, l)) := \max\{|\mathbf{x} - \mathbf{x}_0|^l : \mathbf{x} \in \Omega\}$ . The Lipschitz constant  $L$  satisfying (2.12), which is required for obtaining  $\beta$ , is estimated as follows:

$$\begin{aligned} \|f'_v - f'_w\|_{\mathcal{L}(H_0^1, H^{-1})} &\leq p \sup_{0 \neq \phi \in H_0^1} \sup_{0 \neq \psi \in H_0^1} \frac{|\int_{\Omega} |\mathbf{x} - \mathbf{x}_0|^l (|v(\mathbf{x})|^{p-1} \phi(\mathbf{x}) - |w(\mathbf{x})|^{p-1} \phi(\mathbf{x})) \psi(\mathbf{x}) d\mathbf{x}|}{\|\phi\|_{H_0^1} \|\psi\|_{H_0^1}} \\ &\leq pd \sup_{0 \neq \phi \in H_0^1} \sup_{0 \neq \psi \in H_0^1} \frac{|\int_{\Omega} (|v(\mathbf{x})|^{p-1} - |w(\mathbf{x})|^{p-1}) \phi(\mathbf{x}) \psi(\mathbf{x}) d\mathbf{x}|}{\|\phi\|_{H_0^1} \|\psi\|_{H_0^1}}. \end{aligned} \quad (2.22)$$

Using the mean value theorem, the numerator of (2.22) is evaluated as

$$\begin{aligned}
& \left| \int_{\Omega} (|v(\mathbf{x})|^{p-1} - |w(\mathbf{x})|^{p-1}) \phi(\mathbf{x}) \psi(\mathbf{x}) d\mathbf{x} \right| \\
&= \left| \int_{\Omega} \int_0^1 (p-1) \text{sign}(w(\mathbf{x}) + t(v(\mathbf{x}) - w(\mathbf{x}))) |w(\mathbf{x}) + t(v(\mathbf{x}) - w(\mathbf{x}))|^{p-2} dt \right. \\
&\quad \left. (v(\mathbf{x}) - w(\mathbf{x})) \phi(\mathbf{x}) \psi(\mathbf{x}) d\mathbf{x} \right| \\
&= (p-1) \left| \int_0^1 \int_{\Omega} \text{sign}(w(\mathbf{x}) + t(v(\mathbf{x}) - w(\mathbf{x}))) |w(\mathbf{x}) + t(v(\mathbf{x}) - w(\mathbf{x}))|^{p-2} \right. \\
&\quad \left. (v(\mathbf{x}) - w(\mathbf{x})) \phi(\mathbf{x}) \psi(\mathbf{x}) d\mathbf{x} dt \right| \\
&\leq (p-1) \int_0^1 \|tv + (1-t)w\|_{L^{p+1}}^{p-2} \|v - w\|_{L^{p+1}} \|\phi\|_{L^{p+1}} \|\psi\|_{L^{p+1}} dt \\
&\leq (p-1) C_{p+1}^3 \int_0^1 \|tv + (1-t)w\|_{L^{p+1}}^{p-2} dt \|v - w\|_{H_0^1} \|\phi\|_{H_0^1} \|\psi\|_{H_0^1} \\
&\leq (p-1) C_{p+1}^3 \max\{\|v\|_{L^{p+1}}, \|w\|_{L^{p+1}}\}^{p-2} \|v - w\|_{H_0^1} \|\phi\|_{H_0^1} \|\psi\|_{H_0^1},
\end{aligned}$$

for all  $0 \neq \phi, \psi \in H_0^1(\Omega)$ . Therefore, we have

$$L \leq p(p-1) dC_{p+1}^3 \max\{\|v\|_{L^{p+1}}, \|w\|_{L^{p+1}}\}^{p-2}.$$

Choosing  $v, w$  from  $D = B(\hat{u}, r)$ ,  $r = 2\alpha + \delta$  for small  $\delta > 0$ , we can express them as

$$\begin{cases} v = \hat{u} + r\eta, & \|\eta\|_{H_0^1} \leq 1, \\ w = \hat{u} + r\xi, & \|\xi\|_{H_0^1} \leq 1. \end{cases}$$

Hence, it follows that

$$\begin{aligned}
L &\leq p(p-1) dC_{p+1}^3 \max\{\|\hat{u} + r\eta\|_{L^{p+1}}, \|\hat{u} + r\xi\|_{L^{p+1}}\}^{p-2} \\
&\leq p(p-1) dC_{p+1}^3 (\|\hat{u}\|_{L^{p+1}} + C_{p+1}r)^{p-2}. \tag{2.23}
\end{aligned}$$

## 2.5 Numerical results

In this section, we present numerical results where the existence of solutions of (2.1) was proved for  $p = 3$  on the domains  $\Omega = (0, 1)^N$  ( $N = 1, 2$ ) via the method presented in Sections 2.3 and 2.4. All computations were implemented on a computer with 2.20 GHz Intel Xeon E7-4830 CPUs  $\times$  4, 2 TB RAM, and CentOS 7 using MATLAB 2019b with GCC Version 6.3.0. All rounding errors were strictly estimated using the toolboxes kv Library [22] Version 0.4.49 and Intlab Version 11 [15]. Therefore, the accuracy of all results was guaranteed mathematically. We constructed approximate solutions of (2.1) from a Legendre polynomial basis discussed in [21]. Specifically, we constructed approximate solutions  $\hat{u}$  using the basis functions  $\phi_n$  ( $n = 1, 2, 3, \dots$ ) defined by

$$\begin{aligned}
\phi_n(x) &= \frac{1}{n(n+1)} x(1-x) \frac{dQ_n}{dx}(x) \\
&\text{with } Q_n(x) = \frac{(-1)^n}{n!} \left(\frac{d}{dx}\right)^n x^n (1-x)^n, \quad n = 1, 2, 3, \dots \tag{2.24}
\end{aligned}$$

### 2.5.1 Numerical results on the unit line-segment

To apply our method to  $\Omega = (0, 1)$ , we define the finite-dimensional subspace  $V_M$  of  $H_0^1(\Omega)$  as

$$V_M := \left\{ \sum_{i=1}^M u_i \phi_i(x) : u_i \in \mathbb{R} \right\},$$

where  $2 \leq M < \infty$ . We computed approximate solutions  $\hat{u} \in V_M$  by solving the problem of the matrix equation

$$\text{Find } \hat{u} \in V_M \text{ s.t. } (\nabla \hat{u}, \nabla v_M)_{L^2} = (f(\hat{u}), v_M)_{L^2} \text{ for all } v_M \in V_M \quad (2.25)$$

using the usual Newton method. When we look for a symmetric solution, we restrict the solution space and its finite-dimensional subspace. The following subspace  $V^1$  of  $H_0^1(\Omega)$  is endowed with the same topology

$$V^1 := \left\{ u \in H_0^1(\Omega) : u \text{ is symmetric with respect to } x = \frac{1}{2} \right\}. \quad (2.26)$$

Then, we define the finite-dimensional subspace  $V_M^1$  ( $M \geq 2$ ) of  $V^1$  as

$$V_M^1 := \left\{ \sum_{\substack{i=1 \\ i \text{ is odd}}}^M u_i \phi_i(x) : u_i \in \mathbb{R} \right\}.$$

The method presented in Sections 2.3 and 2.4 can be directly applied when the function spaces  $H_0^1(\Omega)$  and  $V_M$  are replaced with  $V^1$  and  $V_M^1$ , respectively. This restriction reduces the amount of calculation because the matrices in (2.25) become smaller. Moreover, because eigenfunctions of (2.18) are also restricted to be symmetric, eigenvalues associated with anti-symmetric eigenfunctions drop out of the minimization in (2.14). Therefore, the constant  $K$  can be reduced. The other constants required in the verification process (that is,  $C_p$  and  $\|F(\hat{u})\|_{H^{-1}}$ ) are not affected by the restriction. Using the evaluation (2.23) when  $p = 3$  and  $\Omega = (0, 1)$  with the center  $\mathbf{x}_0 = (1/2)$ , we evaluated the Lipschitz constant  $L$  as

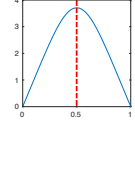
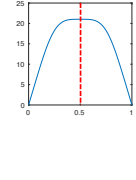
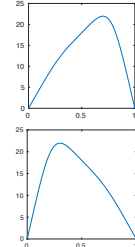
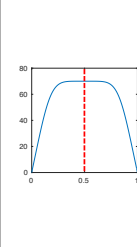
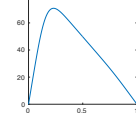
$$L \leq 6 \left( \frac{1}{2} \right)^l C_4^3 (\|\hat{u}\|_{L^4} + C_4 r).$$

Table 2.1 shows the approximate solutions together with their verification results on  $\Omega = (0, 1)$ . The red dashed lines indicate the symmetry of each solution. To satisfy inequality (2.5), our program set  $\tau$  to the next floating-point number after a computed upper bound of the right side of (2.5). Therefore, when  $\hat{u}$  vanishes at some point on  $\bar{\Omega}$ ,  $\tau$  is set to the floating-point number after zero, which is approximately  $4.9407 \times 10^{-324}$ . In Table 2.1,  $\|F(\hat{u})\|_{H^{-1}}$ ,  $\|F'_{\hat{u}}\|_{\mathcal{L}(H^{-1}, H_0^1)}$ ,  $L$ ,  $\alpha$ , and  $\beta$  denote the constants required by Theorem 3. Moreover,  $r_A$  and  $r_R$  denote an upper bound for absolute error  $\|u - \hat{u}\|_{H_0^1}$  and relative error  $\|u - \hat{u}\|_{H_0^1} / \|\hat{u}\|_{H_0^1}$ , respectively. The values in row ‘‘Peak’’ represent upper bounds for the maximum values of the corresponding approximate solutions in decimal form.

The values in rows  $\mu_1-\mu_5$  represent approximations of the five smallest eigenvalues of (2.16) discretized in  $V_{40} \subset H_0^1(\Omega)$ , which is spanned by the basis functions  $\phi_n$  ( $n = 1, 2, \dots, 40$ ) without the restriction of symmetry. When  $l = 2, 4$ , symmetric solutions have two negative eigenvalues and asymmetric solutions have one negative eigenvalue.

Our approximate computation obtained Figure 2.1, the solution curve of (2.1) for  $0 \leq l \leq 8$  ( $l$  is always a multiple of 0.05). The verified points where  $l = 0, 2, 4$  lie on the solution curves. According to Figure 2.1, a bifurcation point is expected to exist around  $[1.20, 1.25]$ .

Table 2.1 Verification results for  $l = 0, 2, 4$  on  $\Omega = (0, 1)$ .

$l$	0	2		4	
$\hat{u}$					
Solution space	$V^1$	$V^1$	$V$	$V^1$	$V$
$M_u$	40	40	40	40	40
$M$	40	40	40	40	40
$\ F(\hat{u})\ _{H^{-1}}$	2.95468e-12	8.35842e-8	4.03869e-6	9.25374e-6	3.36995e-4
$\ F'_{\hat{u}}{}^{-1}\ _{\mathcal{L}(H^{-1}, H_0^1)}$	2.02207	4.19470	3.25043	1.82276	2.16009
$L$	1.28660	2.04106	1.89034	1.78289	1.47489
$\alpha$	5.97456e-12	3.50610e-7	1.31275e-5	1.68674e-5	7.27937e-4
$\beta$	2.60158	8.56162	6.14441	3.24977	3.18587
$r_A$	6.04051e-12	4.15274e-7	1.51947e-5	2.06429e-5	9.27220e-4
$r_R$	7.60887e-13	7.72615e-9	2.89288e-7	1.00215e-7	4.97806e-6
Peak	3.70815	21.0522	22.0954	70.3607	71.2910
$\mu_1$	-1.99999	-2.00000	-1.99999	-1.99999	-1.99999
$\mu_2$	0.500000	-0.238397	0.356085	-0.657337	0.588997
$\mu_3$	0.800001	0.703809	0.679874	0.671403	0.755696
$\mu_4$	0.892858	0.783274	0.865471	0.733254	0.859840
$\mu_5$	0.933334	0.894429	0.910538	0.880449	0.924964

Solution space:  $V := H_0^1(\Omega)$  and the subspace  $V^1$  is defined by (2.26)

$M_u$ : number of basis functions for constructing approximate solution  $\hat{u} \in V_{M_u}$  or  $\hat{u} \in V_{M_u}^1$

$M$ : number of basis functions for calculating  $\lambda^M$

$\|F(\hat{u})\|_{H^{-1}}$ : upper bound for the residual norm estimated via (2.13)

$\|F'_{\hat{u}}{}^{-1}\|_{\mathcal{L}(H^{-1}, H_0^1)}$ : upper bound for the inverse operator norm estimated via Theorem 4

$L$ : upper bound for Lipschitz constant satisfying (2.12)

$\alpha$ : upper bound for  $\alpha$  required in Theorem 3

$\beta$ : upper bound for  $\beta$  required in Theorem 3

$r_A$ : upper bound for absolute error  $\|u - \hat{u}\|_{H_0^1}$

$r_R$ : upper bound for relative error  $\|u - \hat{u}\|_{H_0^1} / \|\hat{u}\|_{H_0^1}$

Peak: upper bound for the maximum values of the corresponding approximation

$\mu_1-\mu_5$ : approximations of the five smallest eigenvalues of (2.16)

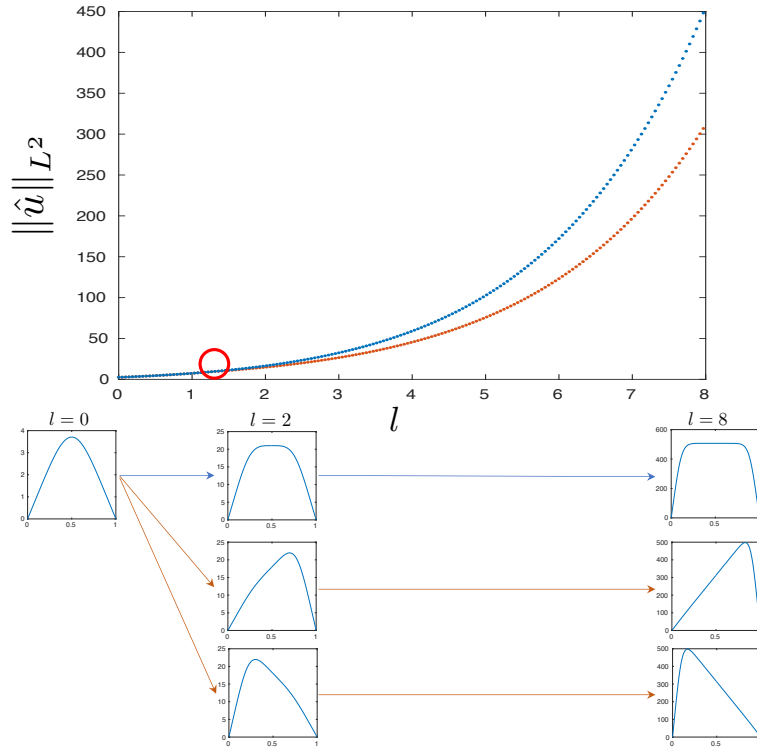


Figure 2.1 Solution curves for (2.1) on the unit line segment (0, 1).

### 2.5.2 Numerical results on the unit square

We apply our method to  $\Omega = (0, 1)^2$  in this subsection. As in Subsection 2.5.1, we again restrict solution spaces and their finite-dimensional subspaces to look for symmetric solutions. The following sub-solution spaces of  $H_0^1(\Omega)$  are endowed with the same topology:

$$\begin{aligned}
 V^1 &:= \left\{ u \in H_0^1(\Omega) : u \text{ is symmetric with respect to } x = \frac{1}{2} \right\}, \\
 V^2 &:= \left\{ u \in H_0^1(\Omega) : u \text{ is symmetric with respect to } y = x \right\}, \\
 V^3 &:= \left\{ u \in H_0^1(\Omega) : u \text{ is symmetric with respect to } y = x \text{ and } y = -x + 1 \right\}, \\
 V^4 &:= \left\{ u \in H_0^1(\Omega) : u \text{ is symmetric with respect to } x = \frac{1}{2}, y = \frac{1}{2}, y = x, \text{ and } y = -x + 1 \right\}.
 \end{aligned}$$



Then, using  $\phi_i$  defined in (2.24), we construct finite-dimensional subspaces  $V_M^i$  ( $M \geq 2$ ) for each  $V^i$  ( $i = 1, 2, 3, 4$ ) as

$$\begin{aligned} V_M^1 &:= \left\{ \sum_{\substack{i=1 \\ i \text{ is odd}}}^M \sum_{j=1}^M u_{i,j} \phi_i(x) \phi_j(y) : u_{i,j} \in \mathbb{R} \right\}, \\ V_M^2 &:= \left\{ \sum_{i=1}^M \sum_{j=i}^M u_{i,j} \psi_{i,j}(x, y) : u_{i,j} \in \mathbb{R} \right\}, \\ V_M^3 &:= \left\{ \sum_{\substack{i=1 \\ i \text{ is odd}}}^M \sum_{\substack{j=i \\ j \text{ is odd}}}^M u_{i,j} \psi_{i,j}(x, y) + \sum_{\substack{i=2 \\ i \text{ is even}}}^M \sum_{\substack{j=i \\ j \text{ is even}}}^M u_{i,j} \psi_{i,j}(x, y) : u_{i,j} \in \mathbb{R} \right\}, \\ V_M^4 &:= \left\{ \sum_{\substack{i=1 \\ i \text{ is odd}}}^M \sum_{\substack{j=i \\ j \text{ is odd}}}^M u_{i,j} \psi_{i,j}(x, y) : u_{i,j} \in \mathbb{R} \right\}, \end{aligned}$$

where  $\psi_{i,j}$  is defined as

$$\psi_{i,j}(x, y) := \phi_i(x)\phi_j(y) + \phi_j(x)\phi_i(y), \quad (x, y) \in \Omega,$$

which is symmetric with respect to the line  $y = x$ . Note that we use the same notation  $V^1$  and  $V_M^1$  with different meanings than in Subsection 2.5.1. The method presented in Sections 2.3 and 2.4 can be directly applied when the function spaces  $H_0^1(\Omega)$  and  $V_M$  are replaced with  $V^i$  and  $V_M^i$ , respectively. In the solution space  $V_M^i$ , approximate solutions  $\hat{u}$  were obtained by solving the matrix equation

$$\text{Find } \hat{u} \in V_M^i \text{ s.t. } (\nabla \hat{u}, \nabla v_M)_{L^2} = (f(\hat{u}), v_M)_{L^2} \quad \text{for all } v_M \in V_M^i \quad (2.27)$$

via the usual Newton method. Restricting solution spaces reduces the amount of calculation for the same reasons as described in Subsection 2.5.1. Using the evaluation (2.23) when  $\Omega = (0, 1)^2$  with the center  $\mathbf{x}_0 = (1/2, 1/2)$ , we evaluated the Lipschitz constant  $L$  as

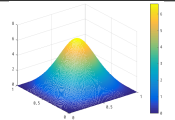
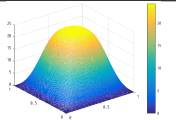
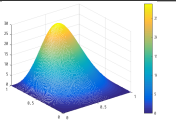
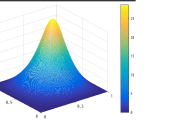
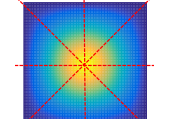
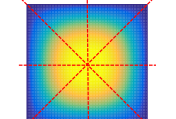
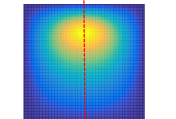
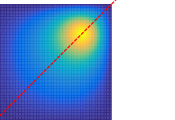
$$L \leq 6 \left( \frac{1}{\sqrt{2}} \right)^l C_4^3 (\|\hat{u}\|_{L^4} + C_4 r).$$

Tables 2.2 and 2.3 show the approximate solutions together with their verification results. The red dashed lines indicate the symmetry of each solution. We again set  $\tau \approx 4.9407 \times 10^{-324}$ , the minimal positive floating-point number after zero. In the tables,  $\|F(\hat{u})\|_{H^{-1}}$ ,  $\|F'_{\hat{u}}\|_{\mathcal{L}(H^{-1}, H_0^1)}$ ,  $L$ ,  $\alpha$ , and  $\beta$  denote the constants required by Theorem 3. Moreover,  $r_A$  and  $r_R$  denote an upper bound for absolute error  $\|u - \hat{u}\|_{H_0^1}$  and relative error  $\|u - \hat{u}\|_{H_0^1} / \|\hat{u}\|_{H_0^1}$ , respectively. The values in row ‘‘Peak’’ represent upper bounds for the maximum values of the corresponding approximate solutions. We see that error bounds are affected by the number of peaks — fewer peaks lead to larger error bounds. As  $l$  increases, the peaks approach the corners of the domain and become higher. Therefore, a larger  $l$  makes verification based on Theorem 3 more difficult. We succeeded in proving the existence of solutions in all cases in which  $l = 0, 2, 4$ , including three-peak solutions not found in [6].

The values in rows  $\mu_1$ – $\mu_5$  represent approximations of the five smallest eigenvalues of (2.16) discretized in  $V_{30} \subset H_0^1(\Omega)$ , which is spanned by the basis functions  $\phi_n$  ( $n = 1, 2, \dots, 30$ ) without the restriction of symmetry. When  $l = 4$ , the number of negative eigenvalues  $\mu$  coincides with the number of peaks.

Our approximate computation obtained Figure 2.2, the solution curves of (2.1) for  $0 \leq l \leq 8$  ( $l$  is always a multiple of 0.05). If the vertical axis scaling is changed, the curves coincide with those in [6, Figure 2] except for that corresponding to the three-peak solutions after the point around [2.35, 2.40]. The verified points where  $l = 0, 2, 4$  lie on the solution curves. According to Figure 2.2, two bifurcation points are expected to exist around [0.55, 0.60] and [2.35, 2.40]. We expect the single-solution curve bifurcates to three at the first bifurcation point around [0.55, 0.60], and then one of them further bifurcates to three at the second point around [2.35, 2.40].

Table 2.2 Verification results for  $l = 0, 2$  on the unit square  $(0, 1)^2$ .

$l$	0	2		
3D $\hat{u}$				
2D $\hat{u}$				
Solution space	$V^4$	$V^4$	$V^1$	$V^2$
$M_u$	40	40	60	60
$M$	40	40	40	40
$\ F(\hat{u})\ _{H^{-1}}$	1.17370e-7	3.96407e-7	1.19312e-8	4.22257e-7
$\ F'_{\hat{u}}{}^{-1}\ _{\mathcal{L}(H^{-1}, H_0^1)}$	1.70326	2.26200	15.19763	36.47472
$L$	6.78398e-1	1.64252	1.43209	1.21150
$\alpha$	1.99910e-7	8.96672e-7	1.81325e-7	1.54017e-5
$\beta$	1.15549	3.71537	21.76424	44.18887
$r_A$	4.63296e-8	2.55597e-7	1.44557e-7	2.48634e-5
$r_R$	3.76958e-9	3.98528e-9	2.45351e-9	4.63166e-7
Peak	6.62326	24.36528	29.03437	29.20268
$\mu_1$	-1.99999	-1.99999	-1.99999	-1.99999
$\mu_2$	0.220034	-0.410090	-0.273589	0.196622
$\mu_3$	0.220034	-0.410090	0.233061	0.208937
$\mu_4$	0.604521	0.114826	0.457439	0.585268
$\mu_5$	0.658421	0.298974	0.517021	0.639470

Solution space: restricted solution space  $V^i \subset H_0^1(\Omega)$

$M_u$ : number of basis functions with respect to  $x$  and  $y$  for constructing approximate solution  $\hat{u} \in V_{M_u}^i$

$M$ : number of basis functions with respect to  $x$  and  $y$  for calculating  $\lambda^M$

$\|F(\hat{u})\|_{H^{-1}}$ : upper bound for the residual norm estimated via (2.13)

$\|F'_{\hat{u}}{}^{-1}\|_{\mathcal{L}(H^{-1}, H_0^1)}$ : upper bound for the inverse operator norm estimated via Theorem 4

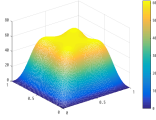
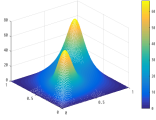
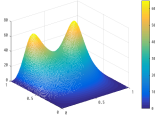
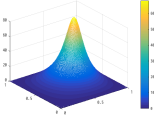
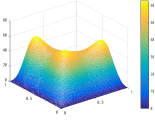
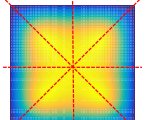
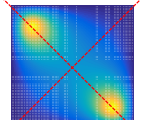
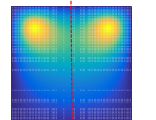
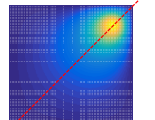
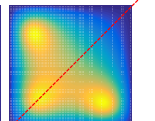
$L$ : upper bound for Lipschitz constant satisfying (2.12)

$\alpha$ : upper bound for  $\alpha$  required in Theorem 3

$\beta$ : upper bound for  $\beta$  required in Theorem 3

$r_A$ : upper bound for absolute error  $\|u - \hat{u}\|_{H_0^1}$   
 $r_R$ : upper bound for relative error  $\|u - \hat{u}\|_{H_0^1} / \|\hat{u}\|_{H_0^1}$   
 Peak: upper bound for the maximum values of the corresponding approximation  
 $\mu_1 - \mu_5$ : approximations of the five smallest eigenvalues of (2.16)

Table 2.3 Verification results for  $l = 4$  on the unit square  $(0, 1)^2$ .

$l$	4				
3D $\hat{u}$					
2D $\hat{u}$					
Solution space	$V^4$	$V^3$	$V^1$	$V^2$	$V^2$
$M_u$	70	70	70	70	70
$M$	80	80	80	80	80
$\ F(\hat{u})\ _{H^{-1}}$	1.88534e-11	7.91070e-6	4.76970e-7	8.47044e-6	3.47384e-8
$\ F_{\hat{u}}'^{-1}\ _{\mathcal{L}(H^{-1}, H_0^1)}$	6.82420	24.18779	78.96665	21.26750	47.44875
$L$	2.31308	1.46531	1.55126	1.18832	1.97091
$\alpha$	1.28659e-10	1.91343e-4	3.76648e-5	1.80145e-4	1.64830e-6
$\beta$	15.78486	35.44250	1.22498e+2	25.27251	93.51720
$r_A$	4.95952e-11	1.73351e-4	8.76586e-5	1.53306e-4	2.32064e-6
$r_R$	2.35369e-13	9.86681e-7	5.12219e-7	1.20925e-6	1.16657e-8
Peak	62.30489	68.15045	66.28947	69.69524	64.16408
$\mu_1$	-1.99999	-1.99996	-1.99999	-1.99999	-1.99999
$\mu_2$	-0.995156	-1.86714	-1.64594	0.177691	-1.46267
$\mu_3$	-0.995156	0.166245	0.130875	0.251043	-1.14006
$\mu_4$	-0.689431	0.205039	0.253364	0.591950	0.131828
$\mu_5$	0.210478	0.258004	0.272595	0.658008	0.175494

Solution space: restricted solution space  $V^i \subset H_0^1(\Omega)$

$M_u$ : number of basis functions with respect to  $x$  and  $y$  for constructing approximate solution  $\hat{u} \in V_{M_u}^i$

$M$ : number of basis functions with respect to  $x$  and  $y$  for calculating  $\lambda^M$

$\|F(\hat{u})\|_{H^{-1}}$ : upper bound for the residual norm estimated via (2.13)

$\|F_{\hat{u}}'^{-1}\|_{\mathcal{L}(H^{-1}, H_0^1)}$ : upper bound for the inverse operator norm estimated via Theorem 4

$L$ : upper bound for Lipschitz constant satisfying (2.12)

$\alpha$ : upper bound for  $\alpha$  required in Theorem 3

$\beta$ : upper bound for  $\beta$  required in Theorem 3

$r_A$ : upper bound for absolute error  $\|u - \hat{u}\|_{H_0^1}$

$r_R$ : upper bound for relative error  $\|u - \hat{u}\|_{H_0^1} / \|\hat{u}\|_{H_0^1}$

Peak: upper bound for the maximum values of the corresponding approximation

$\mu_1 - \mu_5$ : approximations of the five smallest eigenvalues of (2.16)

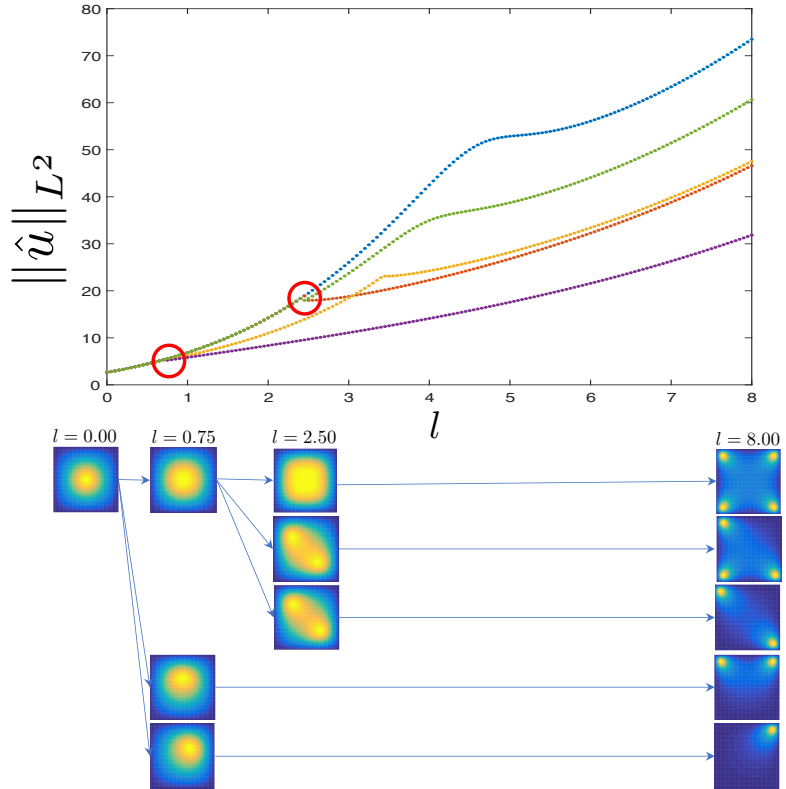


Figure 2.2 Solution curves for (2.1) on the unit square  $(0, 1)^2$ .

## 2.6 Short summary of chapter 2

We designed a numerical verification method for proving the existence of solutions of the Hénon equation (2.1) on a bounded domain based on the Newton-Kantorovich theorem. We applied our method to the domains  $\Omega = (0, 1)^N$  ( $N = 1, 2$ ), proving the existence of several solutions of (2.1) nearby a numerically computed approximation  $\hat{u}$ . In particular, we found a set of undiscovered solutions with three peaks on the square domain  $\Omega = (0, 1)^2$ . Approximate computations generated the solution curves of (2.1) for  $0 \leq l \leq 8$  in Figures 2.1 and 2.2. Our next goal should verify the existence of solutions for arbitrary  $l \in [0, a]$ , given a large  $a > 0$ , and prove the bifurcation structure for (2.1) in a strict mathematical sense. Next chapter, we introduce the method and results verifying the branches and bifurcation points of symmetry-breaking bifurcation for the one-dimensional Hénon equation (2.1).

## Chapter 3

# Advanced numerical verification method and analysis of bifurcation phenomena of the Hénon equation

### 3.1 Introduction

The Hénon equation was proposed as a differential equation describing the density distribution of celestial bodies [1]. And some papers [4, 5, 6, 7, 8, 9] have discussed the Dirichlet boundary value problem

$$\begin{cases} -\Delta u = |\mathbf{x} - \mathbf{x}_0|^l |u|^{p-1} u & \text{in } \Omega, \\ u = 0 & \text{on } \partial\Omega, \end{cases} \quad (3.1)$$

where  $\Omega \subset \mathbb{R}^N$  ( $N = 1, 2, 3$ ) is a bounded domain. Particularly,  $\mathbf{x}_0$  is set at the center of the domain. The real parameter  $l \geq 0$  is the potential index, and the real parameter  $2 \leq p < p^*$  ( $p^* = \infty$  if  $N = 1, 2$  and  $p^* = 5$  if  $N = 3$ ) is the polytropic index. In this chapter, we consider the one-dimensional Hénon equation which is the two-point boundary value problem

$$\begin{cases} -u'' = |x|^l |u|^{p-1} u, & x \in (-1, 1), \\ u(-1) = u(1) = 0, \end{cases} \quad (3.2)$$

where  $l \geq 0, 2 \leq p < \infty$ . It is known that if  $l = 0$ , then there is no asymmetric positive solution [23, 24, 25], and if  $l > 0$  is sufficiently large, then there are some asymmetric solutions [26, 27, 28, 29]. Recent interest in the symmetry-breaking phenomena has spurred a great deal of mathematical research into the Hénon equation over the last decade. S. Tanaka [30, 31] proved that if  $l(p-1) \geq 4$ , the Morse index of the positive least energy solution equals 1 and the Morse index of the positive symmetric solution equals 2, and hence the positive least energy solution is asymmetric and symmetry-breaking phenomena occur. It is also shown that if  $l$  and  $p$  are sufficiently small, then there is no positive asymmetric solution and the Morse index of the symmetric positive solution equals 1. However, still only sufficient conditions for symmetry-breaking bifurcation have been clarified, and the existence of multiple solutions near the bifurcation point and the structure of the bifurcation are not known completely.

The purpose of our study was to verify the existence of multiple solutions of (3.2) near the bifurcation point, and tracking the bifurcation diagrams by computer assis-

tance. Due to the variable coefficient  $|x|^l$  in the problem (3.2), the solution  $u$  has a singularity at  $x = 0$ . We design a numerical verification method that follows such an internal singularity. By applying the method, the existence of multiple solutions can be proved efficiently. As a result, we succeeded in verifying the branches and bifurcation points of the simple symmetry-breaking bifurcation (see Figure 3.1).

The remainder of this chapter is organized as follows. Some notation is introduced in Section 3.2. Sections 3.3 and 3.4 describe numerical verification based on the Newton–Kantorovich theorem together with evaluations of several required constants. Section 3.5 shows the consideration of singularity. Subsequently, Section 3.6 shows the results numerically proving the existence of several solutions of (3.2) using the method that follows an internal singularity. Sections 3.7 and 3.8 show the numerical verification method and results for the branches of (3.2). Sections 3.9 and 3.10 show the numerical verification method and results for the bifurcation point of (3.2).

### 3.2 Preliminaries

We begin by introducing some notation. For two Banach spaces  $X$  and  $Y$ , the set of bounded linear operators from  $X$  to  $Y$  is denoted by  $\mathcal{L}(X, Y)$ . The norm of  $T \in \mathcal{L}(X, Y)$  is defined by

$$\|T\|_{\mathcal{L}(X, Y)} := \sup_{0 \neq u \in X} \frac{\|Tu\|_Y}{\|u\|_X}. \quad (3.3)$$

Let  $L^p(\Omega)$  ( $1 \leq p < \infty$ ) be the function space of  $p$ -th power Lebesgue integrable functions over a domain  $\Omega$  with the  $L^p$ -norm  $\|u\|_{L^p} := (\int_{\Omega} |u(x)|^p dx)^{1/p} < \infty$ . When  $p = 2$ ,  $L^2(\Omega)$  is the Hilbert space with the inner product  $(u, v)_{L^2} := \int_{\Omega} u(x)v(x)dx$ . Let  $L^\infty(\Omega)$  be the function space of Lebesgue measurable functions over  $\Omega$ , with the norm  $\|u\|_{L^\infty} := \text{ess sup}\{|u(x)| : x \in \Omega\}$  for  $u \in L^\infty(\Omega)$ . We denote the first-order  $L^2$  Sobolev space in  $\Omega$  as  $H^1(\Omega)$  and define

$$H_0^1(\Omega) := \{u \in H^1(\Omega) : u = 0 \text{ on } \partial\Omega \text{ in the trace sense}\}$$

as the solution space for the target equation (3.1). We endow  $H_0^1(\Omega)$  with the inner product and norm

$$(u, v)_{H_0^1} := (u', v')_{L^2} + \tau(u, v)_{L^2}, \quad u, v \in H_0^1(\Omega), \quad (3.4)$$

$$\|u\|_{H_0^1} := \sqrt{(u, u)_{H_0^1}}, \quad u \in H_0^1(\Omega), \quad (3.5)$$

where  $\tau$  is a nonnegative number chosen as

$$\tau > -p|x|^l|\hat{u}(x)|^{p-1} \quad \text{a.e. } x \in \Omega \quad (3.6)$$

for a numerically computed approximation  $\hat{u} \in H_0^1(\Omega)$ . The condition (3.6) is required in Subsection 3.4.2 and  $\hat{u}$  is explicitly constructed in Section 3.6. Because the norm  $\|\cdot\|_{H_0^1}$  monotonically increases with respect to  $\tau$ , the  $H_0^1(\Omega)$  norm  $\|\cdot\|_{L^2}$  is dominated by the norm  $\|\cdot\|_{H_0^1}$  for all  $\tau \geq 0$ . Therefore, the error bound  $\|u - \hat{u}\|_{H_0^1}$  is always an upper bound for  $\|(u - \hat{u})'\|_{L^2}$ . The topological dual space of  $H_0^1(\Omega)$  is denoted by  $H^{-1}$  with the usual supremum norm defined in (3.3).

The bound for the embedding  $H_0^1(\Omega) \hookrightarrow L^p(\Omega)$  is denoted by  $C_p$  ( $p \geq 2$ ). More precisely,  $C_p$  is a positive number satisfying

$$\|u\|_{L^p} \leq C_p \|u\|_{H_0^1} \quad \text{for all } u \in H_0^1(\Omega). \quad (3.7)$$

Note that  $\|u\|_{H^{-1}} \leq C_p \|u\|_{L^q}$ ,  $u \in L^q(\Omega)$  holds for  $q$  satisfying  $p^{-1} + q^{-1} = 1$ . Explicitly estimating the embedding constant  $C_p$  is important for our numerical verification. When  $p = 2$ , we use the following optimal inequality:

$$\|u\|_{L^2} \leq \frac{1}{\sqrt{\lambda_1 + \tau}} \|u\|_{H_0^1},$$

where  $\lambda_1$  is the first eigenvalue of the minus Laplacian in the weak sense. Especially when  $\Omega = (-1, 1)$ , we have  $\lambda_1 = \pi^2/4$ . When  $p$  is not 2, we use the following theorems depending on the dimension of  $\Omega$ . We use [10, Lemma 7.12] to obtain an explicit value of  $C_p$  for a one-dimensional bounded domain.

**Theorem 7** ([10, Lemma 7.12]) *Let  $\Omega = (a, b) \subset \mathbb{R}$ , with  $a \in \mathbb{R} \cup \{-\infty\}$ ,  $b \in \mathbb{R} \cup \{+\infty\}$ ,  $a < b$ . Moreover, let  $\rho^*$  denote the minimal point of the spectrum of  $-u''$  on  $H_0^1(\Omega)$ , i.e.  $\rho^* = \pi^2/(b-a)^2$  if  $(a, b)$  is bounded. Then, for all  $u \in H_0^1(\Omega)$ ,*

$$\|u\|_{L^p} \leq C_p \|u\|_{H_0^1} \quad (p \in (2, \infty)),$$

where, abbreviating  $\varepsilon := \frac{2}{p} \in (0, 1)$ ,

$$C_p := \begin{cases} \frac{1}{\sqrt{2}}(1-\varepsilon)^{\frac{1}{4}(1-\varepsilon)}(1+\varepsilon)^{\frac{1}{4}(1+\varepsilon)}\tau^{-\frac{1}{4}(1+\varepsilon)} & \text{if } \rho^* \leq \tau \frac{1-\varepsilon}{1+\varepsilon}, \\ \frac{1}{\sqrt{\rho^* + \tau}}(\rho^*)^{\frac{1}{4}(1-\varepsilon)} & \text{otherwise,} \end{cases}$$

for  $p \in (2, \infty)$ .

### 3.3 Numerical verification method

This section discusses the numerical verification method used in this chapter. We first define the operator  $f$  as

$$f : \begin{cases} u(\cdot) & \mapsto |\cdot|^l |u(\cdot)|^{p-1} u(\cdot), \\ H_0^1(\Omega) & \rightarrow H^{-1}, \end{cases}$$

where  $2 \leq p < p^*$  ( $p^* = \infty$  if  $N = 1, 2$  and  $p^* = 5$  if  $N = 3$ ). Furthermore, we define the nonlinear operator  $F : H_0^1(\Omega) \rightarrow H^{-1}$  by  $F(u) := -u'' - f(u)$ , which is given by

$$\langle F(u), v \rangle = (u', v')_{L^2} - \langle f(u), v \rangle \quad \text{for all } v \in H_0^1(\Omega),$$

where  $\langle f(u), v \rangle = \int_{\Omega} (|x|^l |u(x)|^{p-1} u(x)) v(x) dx$ . The Fréchet derivatives of  $f$  and  $F$  at  $\varphi \in H_0^1(\Omega)$  are denoted by  $f'_\varphi$  and  $F'_\varphi$ , respectively, and given by

$$\langle f'_\varphi u, v \rangle = \int_{\Omega} (p|x|^l |\varphi(x)|^{p-1} u(x)) v(x) dx \quad \text{for all } u, v \in H_0^1(\Omega), \quad (3.8)$$

$$\langle F'_\varphi u, v \rangle = (u', v')_{L^2} - \langle f'_\varphi u, v \rangle \quad \text{for all } u, v \in H_0^1(\Omega). \quad (3.9)$$

Then, we consider the following problem:

$$\text{Find } u \in H_0^1(\Omega) \text{ s.t. } F(u) = 0, \quad (3.10)$$

which is the weak form of the problem (3.2). To conduct the numerical verification for this problem, we apply the Newton–Kantorovich theorem, which enables us to prove the existence of a true solution  $u$  near a numerically computed “good” approximate solution  $\hat{u}$  (see, for example, [12]). Hereafter,  $B(\hat{u}, r)$  and  $\bar{B}(\hat{u}, r)$  respectively denote the open and closed balls with center approximate solution  $\hat{u}$  and radius  $r$  in terms of norm  $\|\cdot\|_{H_0^1}$ .

**Theorem 8 (Newton–Kantorovich’s theorem)** *Let  $\hat{u} \in H_0^1(\Omega)$  be some approximate solution of  $F(u) = 0$ . Suppose that there exists some  $\alpha > 0$  satisfying*

$$\|F'_{\hat{u}}{}^{-1}F(\hat{u})\|_{H_0^1} \leq \alpha. \quad (3.11)$$

Moreover, suppose that there exists some  $\beta > 0$  satisfying

$$\|F'_{\hat{u}}{}^{-1}(F'_v - F'_w)\|_{\mathcal{L}(H_0^1, H_0^1)} \leq \beta \|v - w\|_{H_0^1}, \quad \text{for all } v, w \in D, \quad (3.12)$$

where  $D = B(\hat{u}, 2\alpha + \delta)$  is an open ball depending on the above value  $\alpha > 0$  for small  $\delta > 0$ . If

$$\alpha\beta \leq \frac{1}{2}, \quad (3.13)$$

then there exists a solution  $u \in H_0^1(\Omega)$  of  $F(u) = 0$  in  $\bar{B}(\hat{u}, \rho)$  with

$$\rho = \frac{1 - \sqrt{1 - 2\alpha\beta}}{\beta}.$$

Furthermore, the solution  $u$  is unique in  $\bar{B}(\hat{u}, 2\alpha)$ .

### 3.4 Evaluation for $\alpha$ and $\beta$

To apply Theorem 8 to the numerical verification for problem (3.2), we need to explicitly evaluate  $\alpha$  and  $\beta$ . The left side of (3.11) is evaluated as

$$\|F'_{\hat{u}}{}^{-1}F(\hat{u})\|_{H_0^1} \leq \|F'_{\hat{u}}{}^{-1}\|_{\mathcal{L}(H^{-1}, H_0^1)} \|F(\hat{u})\|_{H^{-1}}.$$

Therefore, we set

$$\alpha = \|F'_{\hat{u}}{}^{-1}\|_{\mathcal{L}(H^{-1}, H_0^1)} \|F(\hat{u})\|_{H^{-1}}.$$

Moreover, the left side of (3.12) is estimated as

$$\begin{aligned} \|F'_{\hat{u}}{}^{-1}(F'_v - F'_w)\|_{\mathcal{L}(H_0^1, H_0^1)} &\leq \|F'_{\hat{u}}{}^{-1}\|_{\mathcal{L}(H^{-1}, H_0^1)} \|F'_v - F'_w\|_{\mathcal{L}(H_0^1, H^{-1})} \\ &= \|F'_{\hat{u}}{}^{-1}\|_{\mathcal{L}(H^{-1}, H_0^1)} \|f'_v - f'_w\|_{\mathcal{L}(H_0^1, H^{-1})}. \end{aligned}$$

Hence, the desired value of  $\beta$  is obtained via

$$\beta \leq \|F'_{\hat{u}}{}^{-1}\|_{\mathcal{L}(H^{-1}, H_0^1)} L,$$



where  $L$  is the Lipschitz constant satisfying

$$\|f'_v - f'_w\|_{\mathcal{L}(H_0^1, H^{-1})} \leq L\|v - w\|_{H_0^1} \quad \text{for all } v, w \in D. \quad (3.14)$$

We are left to evaluate the inverse operator norm  $\|F'_{\hat{u}}{}^{-1}\|_{\mathcal{L}(H^{-1}, H_0^1)}$ , the residual norm  $\|F(\hat{u})\|_{H^{-1}}$ , and the Lipschitz constant  $L$  for problem (3.10).

### 3.4.1 Residual norm $\|F(\hat{u})\|_{H^{-1}}$

If the approximation  $\hat{u}$  is sufficiently smooth so that  $\hat{u}'' \in L^2(\Omega)$ , we can evaluate the residual norm  $\|F(\hat{u})\|_{H^{-1}}$  as follows:

$$\|F(\hat{u})\|_{H^{-1}} \leq C_2\|\hat{u}'' + f(\hat{u})\|_{L^2}, \quad (3.15)$$

where  $C_2$  is the embedding constant satisfying (3.7) for  $p = p' = 2$ . Our numerical experiments discussed in Section 3.6 use this evaluation, calculating the  $L^2$ -norm via stable numerical integration with all rounding errors strictly estimated.

However, the condition  $\hat{u}'' \in L^2(\Omega)$  is not satisfied such as when we construct  $\hat{u}$  with a piecewise linear finite element basis. We use the method of [10, Subsection 7.2] to evaluate the residual norm applicable to such a case. The following is a brief description of the evaluation method. First, we find an approximation  $\rho \in H(\text{div}, \Omega) = \{\tau \in L^2(\Omega)^N : \text{div } \tau \in L^2(\Omega)\}$  to  $\hat{u}'$ . Then, the residual norm is evaluated as

$$\begin{aligned} \|F(\hat{u})\|_{H^{-1}} &= \|-\hat{u}'' - f(\hat{u})\|_{H^{-1}}, \\ &= \|-\hat{u}'' + \text{div } \rho - \text{div } \rho - f(\hat{u})\|_{H^{-1}}, \\ &\leq \|\text{div}(-\hat{u}' + \rho)\|_{H^{-1}} + \|\text{div } \rho + f(\hat{u})\|_{H^{-1}}, \\ &\leq \|-\hat{u}' + \rho\|_{L^2} + C_2\|\text{div } \rho + f(\hat{u})\|_{L^2}, \end{aligned}$$

where we used  $\|\text{div } \omega\|_{H^{-1}} \leq \|\omega\|_{L^2}$  for  $\omega \in H(\text{div}, \Omega)$ . As mentioned in [10, Subsection 7.2],  $\rho$  can be computed without additional computational resources when we use the mixed finite element method to construct  $\hat{u}$ .

### 3.4.2 Inverse operator norm $\|F'_{\hat{u}}{}^{-1}\|_{\mathcal{L}(H^{-1}, H_0^1)}$

In this subsection, we evaluate the inverse operator norm  $\|F'_{\hat{u}}{}^{-1}\|_{\mathcal{L}(H^{-1}, H_0^1)}$ . To this end, we use the following theorem.

**Theorem 9 ([13])** *Let  $\Phi : H_0^1(\Omega) \rightarrow H^{-1}$  be the canonical isometric isomorphism; that is,  $\Phi$  is given by*

$$\langle \Phi u, v \rangle := (u, v)_{H_0^1} \quad \text{for } u, v \in H_0^1(\Omega).$$

If

$$\mu_0 := \min \{|\mu| : \mu \in \sigma_p(\Phi^{-1}F'_{\hat{u}}) \cup \{1\}\} \quad (3.16)$$

is positive, then the inverse of  $F'_{\hat{u}}$  exists, and we have

$$\|F'_{\hat{u}}{}^{-1}\|_{\mathcal{L}(H^{-1}, H_0^1)} \leq \mu_0^{-1}, \quad (3.17)$$

where  $\sigma_p(\Phi^{-1}F'_{\hat{u}})$  denotes the point spectrum of  $\Phi^{-1}F'_{\hat{u}}$ .

The eigenvalue problem  $\Phi^{-1}F'_u u = \mu u$  in  $H_0^1(\Omega)$  is equivalent to

$$(u', v')_{L^2} - \langle f'_u u, v \rangle = \mu (u, v)_{H_0^1} \quad \text{for all } v \in H_0^1(\Omega), \quad (3.18)$$

where  $(u, v)_{H_0^1}$  denotes the inner product defined in (3.4) that depends on  $\tau$  and  $\langle f'_u u, v \rangle$  is given by (3.8).

We consider the operator  $\mathcal{N} := \Phi - F'_u$  from  $H_0^1(\Omega)$  to  $H^{-1}$ , which satisfies  $\langle \mathcal{N}u, v \rangle = \int_{\Omega} (p|x|^l|\hat{u}(x)|^{p-1})u(x)v(x)dx$  for all  $u, v \in H_0^1(\Omega)$ . Because  $\mathcal{N}$  maps  $H_0^1(\Omega)$  into  $L^2(\Omega)$  and the embedding  $L^2(\Omega) \hookrightarrow H^{-1}$  is compact,  $\mathcal{N} : H_0^1(\Omega) \rightarrow H^{-1}$  is a compact operator. Therefore,  $F'_u$  is a Fredholm operator, and the spectrum  $\sigma(\Phi^{-1}F'_u)$  of  $\Phi^{-1}F'_u$  is given by

$$\sigma(\Phi^{-1}F'_u) = 1 - \sigma(\Phi^{-1}\mathcal{N}) = 1 - \{\sigma_p(\Phi^{-1}\mathcal{N}) \cup \{0\}\} = \sigma_p(\Phi^{-1}F'_u) \cup \{1\}.$$

Accordingly, it suffices to look for eigenvalues  $\mu \neq 1$ . By setting  $\lambda = (1 - \mu)^{-1}$ , we further transform this eigenvalue problem into

$$\text{Find } u \in H_0^1(\Omega) \text{ and } \lambda \in \mathbb{R} \text{ s.t. } (u, v)_{H_0^1} = \lambda \langle (\tau + f'_u)u, v \rangle \quad \text{for all } v \in H_0^1(\Omega), \quad (3.19)$$

where  $\langle (\tau + f'_u)u, v \rangle = \int_{\Omega} (\tau + p|x|^l|\hat{u}(x)|^{p-1})u(x)v(x)dx$  for  $u, v \in H_0^1(\Omega)$ . Because  $\tau$  is chosen so that  $\tau + f'_u$  becomes positive (see (3.6)), (3.19) is a regular eigenvalue problem, the spectrum of which consists of a sequence  $\{\lambda_k\}_{k=1}^{\infty}$  of eigenvalues converging to  $+\infty$ . To compute  $\|F'_u\|_{\mathcal{L}(H^{-1}, H_0^1)}$  on the basis of Theorem 9, we need to enclose the eigenvalue  $\lambda$  of (3.19) that minimizes the corresponding absolute value of  $|\mu|$  ( $= |1 - \lambda^{-1}|$ ). We consider the approximate eigenvalue problem

$$\text{Find } u_M \in V_M \text{ and } \lambda^M \in \mathbb{R} \text{ s.t. } (u_M, v_M)_{H_0^1} = \lambda^M \langle (\tau + f'_u)u_M, v_M \rangle \quad \text{for all } v_M \in V_M, \quad (3.20)$$

where  $V_M$  is a finite-dimensional subspace of  $H_0^1(\Omega)$  such as the space spanned by the finite element basis and Fourier basis. For our problem,  $V_M$  will be explicitly chosen in Section 3.6. Note that (3.20) is a matrix problem with eigenvalues that can be enclosed with rigorous computation techniques (see, for example, [14, 15, 16]).

We then estimate the error between the  $k$ -th eigenvalue  $\lambda_k$  of (3.19) and the  $k$ -th eigenvalue  $\lambda_k^M$  of (3.20). We consider the weak formulation of the Poisson equation,

$$(u_g, v)_{H_0^1} = (g, v)_{L^2} \quad \text{for all } v \in H_0^1(\Omega) \quad (3.21)$$

given  $g \in L^2(\Omega)$ . This equation has a unique solution  $u_g \in H_0^1(\Omega)$  for each  $g \in L^2(\Omega)$  [17]. Let  $P_M^\tau : H_0^1(\Omega) \rightarrow V_M$  be the orthogonal projection defined by

$$(P_M^\tau u - u, v_M)_{H_0^1} = 0 \quad \text{for all } u \in H_0^1(\Omega) \text{ and } v_M \in V_M.$$

The following theorem enables us to estimate the error between  $\lambda_k$  and  $\lambda_k^M$ .

**Theorem 10 ([18, 19])** *Let  $\hat{u} \in H_0^1(\Omega) \cap L^\infty(\Omega)$ . Suppose that there exists  $C_M^\tau > 0$  such that*

$$\|u_g - P_M^\tau u_g\|_{H_0^1} \leq C_M^\tau \|g\|_{L^2} \quad (3.22)$$

for any  $g \in L^2(\Omega)$  and the corresponding solution  $u_g \in H_0^1(\Omega)$  of (3.21). Then,

$$\frac{\lambda_k^M}{\lambda_k^M (C_M^\tau)^2 \|\tau + f'_u\|_{L^\infty} + 1} \leq \lambda_k \leq \lambda_k^M,$$

where the  $L^\infty$ -norm is defined by  $\|\tau + f'_u\|_{L^\infty} := \text{esssup} \{|\tau + p|x|^l|\hat{u}(x)|^{p-1}| : x \in \Omega\}$ .

The right inequality is known as the Rayleigh–Ritz bound, which is derived from the min-max principle:

$$\lambda_k = \min_{H_k \subset H_0^1(\Omega)} \left( \max_{v \in H_k \setminus \{0\}} \frac{\|v\|_{H_0^1}^2}{\|av\|_{L^2}^2} \right) \leq \lambda_k^M,$$

where  $a(x) = \sqrt{\tau + p|x|^l|\hat{u}(x)|^{p-1}}$ , and the minimum is taken over all  $k$ -dimensional subspaces  $H_k$  of  $H_0^1(\Omega)$ . The left inequality was proved in [18, 19]. Assuming the  $H^2$ -regularity of solutions to (3.21) (which follows, for example, when  $\Omega$  is a convex polygonal domain [17, Section 3.3]), [18, Theorem 4] ensures the left inequality. A more general statement that does not require the  $H^2$ -regularity is proved in [19, Theorem 2.1].

When the solution of (3.21) has  $H^2$ -regularity, (3.22) can be replaced with

$$\|u - P_M^\tau u\|_{H_0^1} \leq C_M^\tau \| -u'' + \tau u \|_{L^2} \quad \text{for all } u \in H^2(\Omega) \cap H_0^1(\Omega). \quad (3.23)$$

The constant  $C_M^\tau$  satisfying (3.23) is obtained as  $C_M^\tau = C_M^0 \sqrt{1 + \tau (C_M^0)^2}$  (see [20, Remark A.4]). For example, when  $\Omega = (-1, 1)$ , an explicit value of  $C_M^0$  is obtained for  $V_M$  spanned by the Legendre polynomial basis using [21, Theorem 2.3]. This will be used for our computation in Section 3.6.

**Theorem 11 ([21])** *When  $\Omega = (-1, 1)$ , the inequality*

$$\|(u - P_M^0 u)'\|_{L^2} \leq C_M^0 \|u''\|_{L^2} \quad \text{for all } u \in H^2(\Omega) \cap H_0^1(\Omega) \quad (3.24)$$

holds for

$$C_M^0 = 2 \max \left\{ \frac{1}{2(2M+1)(2M+5)} + \frac{1}{4(2M+5)\sqrt{2M+3}\sqrt{2M+7}}, \right. \\ \left. \frac{1}{4(2M+5)\sqrt{2M+3}\sqrt{2M+7}} + \frac{1}{2(2M+5)(2M+9)} + \frac{1}{4(2M+9)\sqrt{2M+7}\sqrt{2M+11}} \right\}^{\frac{1}{2}}.$$

### 3.4.3 Lipschitz constant $L$

Hereafter, we denote  $d(= d(\Omega, l)) := \max\{|x|^l : x \in \Omega\}$ . The Lipschitz constant  $L$  satisfying (3.14), which is required for obtaining  $\beta$ , is estimated as follows:

$$\begin{aligned} \|f'_v - f'_w\|_{\mathcal{L}(H_0^1, H^{-1})} &\leq p \sup_{0 \neq \phi \in H_0^1} \sup_{0 \neq \psi \in H_0^1} \frac{|\int_{\Omega} |x|^l (|v(x)|^{p-1} \phi(x) - |w(x)|^{p-1} \phi(x)) \psi(x) dx|}{\|\phi\|_{H_0^1} \|\psi\|_{H_0^1}} \\ &\leq pd \sup_{0 \neq \phi \in H_0^1} \sup_{0 \neq \psi \in H_0^1} \frac{|\int_{\Omega} (|v(x)|^{p-1} - |w(x)|^{p-1}) \phi(x) \psi(x) dx|}{\|\phi\|_{H_0^1} \|\psi\|_{H_0^1}}. \end{aligned} \quad (3.25)$$

Using the mean value theorem, the numerator of (3.25) is evaluated as

$$\begin{aligned}
 & \left| \int_{\Omega} (|v(x)|^{p-1} - |w(x)|^{p-1}) \phi(x) \psi(x) dx \right| \\
 &= \left| \int_{\Omega} \int_0^1 (p-1) \text{sign}(w(x) + t(v(x) - w(x))) |w(x) + t(v(x) - w(x))|^{p-2} dt \right. \\
 & \qquad \qquad \qquad \left. (v(x) - w(x)) \phi(x) \psi(x) dx \right| \\
 &= (p-1) \left| \int_0^1 \int_{\Omega} \text{sign}(w(x) + t(v(x) - w(x))) |w(x) + t(v(x) - w(x))|^{p-2} \right. \\
 & \qquad \qquad \qquad \left. (v(x) - w(x)) \phi(x) \psi(x) dx dt \right| \\
 &\leq (p-1) \int_0^1 \|tv + (1-t)w\|_{L^{p+1}}^{p-2} \|v - w\|_{L^{p+1}} \|\phi\|_{L^{p+1}} \|\psi\|_{L^{p+1}} dt \\
 &\leq (p-1) C_{p+1}^3 \int_0^1 \|tv + (1-t)w\|_{L^{p+1}}^{p-2} dt \|v - w\|_{H_0^1} \|\phi\|_{H_0^1} \|\psi\|_{H_0^1} \\
 &\leq (p-1) C_{p+1}^3 \max\{\|v\|_{L^{p+1}}, \|w\|_{L^{p+1}}\}^{p-2} \|v - w\|_{H_0^1} \|\phi\|_{H_0^1} \|\psi\|_{H_0^1},
 \end{aligned}$$

for all  $0 \neq \phi, \psi \in H_0^1(\Omega)$ . Therefore, we have

$$L \leq p(p-1) dC_{p+1}^3 \max\{\|v\|_{L^{p+1}}, \|w\|_{L^{p+1}}\}^{p-2}.$$

Choosing  $v, w$  from  $D = B(\hat{u}, r)$ ,  $r = 2\alpha + \delta$  for small  $\delta > 0$ , we can express them as

$$\begin{cases} v = \hat{u} + r\eta, & \|\eta\|_{H_0^1} \leq 1, \\ w = \hat{u} + r\xi, & \|\xi\|_{H_0^1} \leq 1. \end{cases}$$

Hence, it follows that

$$\begin{aligned}
 L &\leq p(p-1) dC_{p+1}^3 \max\{\|\hat{u} + r\eta\|_{L^{p+1}}, \|\hat{u} + r\xi\|_{L^{p+1}}\}^{p-2} \\
 &\leq p(p-1) dC_{p+1}^3 (\|\hat{u}\|_{L^{p+1}} + C_{p+1}r)^{p-2}. \tag{3.26}
 \end{aligned}$$

When  $\Omega = (-1, 1)$ , (3.26) is reduced to

$$L \leq p(p-1) C_{p+1}^3 (\|\hat{u}\|_{L^{p+1}} + C_{p+1}r)^{p-2}.$$

### 3.5 Consideration of singularity

Due to the variable coefficient  $|x|^l$  in the problem (3.2), the solution  $u$  has a singularity at  $x = 0$ . Then, we present a numerical verification method that follows such a internal singularity in this section. In general, if the solution  $u$  contains singularity, constructing the approximate solution  $\hat{u}$  with only smooth basis functions results in a large residual. Its large residuals make it difficult to satisfy the condition (3.13) of Newton–Kantorovich’s theorem. An example of dealing with a problem involving singularity is Kobayashi’s research for finite element discretizations in a non-convex domain using singular functions [32]. We apply the technique of using singular functions to our problem with internal singularity. The idea is to construct approximate solutions as

$$\hat{u}(x) = u_0 \phi_0(x) + \sum_{i=1}^{M_u} u_i \phi_i(x), \quad u_i \in \mathbb{R}.$$

by using a singular function  $\phi_0(x)$  and smooth functions sequence  $\phi_n(x)$  ( $n = 1, 2, 3, \dots$ ).

Specifically, we define the finite-dimensional subspace  $V_M$  ( $2 \leq M < \infty$ ) of  $H_0^1(\Omega)$  as

$$V_M := \left\{ u_0 \phi_0(x) + \sum_{i=1}^M u_i \phi_i(x) : u_i \in \mathbb{R} \right\},$$

where, smooth functions  $\phi_n(x)$  ( $n = 1, 2, 3, \dots$ )[21] defined by

$$\begin{aligned} \phi_n(x) &= \frac{1}{n(n+1)}(x+1)(1-x) \frac{dQ_n}{dx}(x) \\ \text{with } Q_n(x) &= \frac{(-1)^n}{n!2^n} \left( \frac{d}{dx} \right)^n (x+1)^n (1-x)^n, \quad n = 1, 2, 3, \dots, \end{aligned} \quad (3.27)$$

and the singular function is defined as  $\phi_0(x) = |x|^{2+l} \phi_1(x)$ . We computed approximate solutions  $\hat{u} \in V_M$  by solving the matrix equation

$$\text{Find } \hat{u} \in V_M \text{ s.t. } (\hat{u}', v_M')_{L^2} = (f(\hat{u}), v_M)_{L^2} \quad \text{for all } v_M \in V_M \quad (3.28)$$

using the usual Newton's method.

**Remark 1** Let  $V_M^0$  be a finite dimensional subspace of  $H_0^1(\Omega)$  such as the space spanned by the Legendre polynomial basis, and let  $V_M := V_M^0 \oplus \{\phi_0\}$  be a finite dimensional subspace of  $H_0^1(\Omega)$  containing singularities, and  $P_M : H_0^1(\Omega) \rightarrow V_M$  be the projection. Since  $V_M^0 \subset V_M$  and

$$\|(u - P_M u)'\|_{L^2} \leq \|(u - P_M^0 u)'\|_{L^2},$$

the constant  $C_M^0$  in (3.24) can be also used for  $C_M$  to evaluate that

$$\|(u - P_M u)'\|_{L^2} \leq C_M \|u''\|_{L^2} \quad \text{for all } u \in H^2(\Omega) \cap H_0^1(\Omega).$$

### 3.5.1 Techniques for computing singular functions

Since we need to calculate for the singular function such as  $\phi_0(x) = |x|^{2+l} \phi_1(x)$ , we defined a "class" that can holds the exponential part  $a$  and the polynomial part  $\mathcal{P}(x)$  of

$$|x|^a \mathcal{P}(x)$$

at the same time. We named the "class" as **fpsa**. The operations are defined as follows.

**fpsa** :

- Addition :  $|x|^a \mathcal{P}_1(x) + |x|^a \mathcal{P}_2(x) = |x|^a (\mathcal{P}_1(x) + \mathcal{P}_2(x))$
- Subtraction :  $|x|^a \mathcal{P}_1(x) - |x|^a \mathcal{P}_2(x) = |x|^a (\mathcal{P}_1(x) - \mathcal{P}_2(x))$
- Mmultiplication :  $|x|^{a_1} \mathcal{P}_1(x) \times |x|^{a_2} \mathcal{P}_2(x) = |x|^{a_1+a_2} (\mathcal{P}_1(x) \times \mathcal{P}_2(x))$
- pow :  $\text{pow}(|x|^a \mathcal{P}(x), b) = |x|^{ab} \mathcal{P}^b(x)$

- First-order derivative :  $|x|^{a-2}(ax\mathcal{P}(x)) + |x|^a\mathcal{P}'(x)$
- Second-order derivative :  $|x|^{a-2}(a(a-1)\mathcal{P}(x)) + |x|^{a-2}(2ax\mathcal{P}'(x)) + |x|^a\mathcal{P}''(x)$
- Integration

In order to deal with the “algebraic type singularity”, the integration is performed as follows.

$$\begin{aligned} \int_{-1}^1 |x|^a \mathcal{P}(x) dx &= \int_{-1}^1 |x|^a (t_0 + t_1 x + \dots + t_n x^n) dx \\ &= \int_0^1 x^a (t_0 + t_1 x + \dots + t_n x^n) dx + \int_{-1}^0 (-x)^a (t_0 + t_1 x + \dots + t_n x^n) dx \\ &= \int_0^1 (t_0 x^a + t_1 x^{1+a} + \dots + t_n x^{n+a}) dx + \int_0^1 (t_0 y^a - t_1 y^{1+a} + \dots + t_n y^{n+a}) dy \\ &= \left[ \frac{t_0}{1+a} x^{1+a} + \frac{t_1}{2+a} x^{2+a} + \dots + \frac{t_n}{n+1+a} x^{n+1+a} \right]_0^1 \\ &\quad + \left[ \frac{t_0}{1+a} y^{1+a} - \frac{t_1}{2+a} y^{2+a} + \dots + \frac{t_n}{n+1+a} y^{n+1+a} \right]_0^1 \end{aligned}$$

However, we could not define the addition between `fpsa` with different exponential part  $a$ , so we defined a “class” as

$$\begin{pmatrix} |x|^{a_1} \mathcal{P}_1(x) \\ \vdots \\ |x|^{a_n} \mathcal{P}_n(x) \end{pmatrix} := |x|^{a_1} \mathcal{P}_1(x) + \dots + |x|^{a_n} \mathcal{P}_n(x)$$

using a vector, which is named `vfpsa`. Here, the derivative of `fpsa` is also held by `vfpsa`. The operations are defined as follows.

`vfpsa` :

- Addition
- Subtraction
- Multiplication
- pow
- First-order derivative
- Second-order derivative
- Integration
- cast function (from `fpsa` to `vfpsa`)

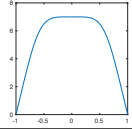
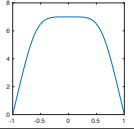
### 3.6 Numerical results of the existence of solutions

In this section, we present numerical results where the existence of solutions of (3.2) was proved for  $p = 3$  via the method presented in Sections 3.3 and 3.4. All computations were implemented on a computer with 2.20 GHz Intel Xeon E7-4830 CPUs  $\times$  4, 2 TB RAM, and CentOS 7 using MATLAB 2019b with GCC Version 6.3.0. All

rounding errors were strictly estimated using the toolboxes kv Library [22] Version 0.4.49 and Intlab Version 11 [15]. Therefore, the accuracy of all results was guaranteed mathematically.

First, we discuss the effects of singular functions. Figure 3.1 shows the comparison with and without singular basis functions. According to the Figure 3.1, if we mixed a singular function  $\phi_0$  to construct approximate solution  $\hat{u}$ , the upper bound for the residual norm falls well enough to satisfy the condition  $\alpha\beta \leq 1/2$ , so we succeeded in verifying the existence of the solution. On the other hand, if we did not mix a singular function  $\phi_0$  to construct approximate solution  $\hat{u}$ , the upper bound for the residual norm does not fall sufficiently, so we failed in verifying the existence of the solution. Furthermore, without a singular function  $\phi_0$ , the residual norm only drops to about  $1.16525e-4$  even when increasing to  $Mu = 100$ . In that case, the residuals do not reach the order of the case with singular functions when  $Mu = 30$ . Therefore, the effect of the singular function is large.

Table 3.1 Verification results for  $p = 3, l = 3$ .

$\phi_0$	○	×
$\hat{u}$		
$M_u$	30	30
$M$	30	30
$\ F(\hat{u})\ _{H^{-1}}$	4.53868e-5	7.75707e-3
$\ F'_{\hat{u}}{}^{-1}\ _{\mathcal{L}(H^{-1}, H_0^1)}$	2.10553	2.10553
$L$	3.22221e+1	3.23520e+1
$\alpha$	9.55632e-5	1.63328e-2
$\beta$	6.78446e+1	6.81181e+1
$\alpha\beta$	6.48344e-3	1.11256
$r_A$	1.22503e-4	fail
$r_R$	8.98750e-6	fail

$M_u$ : number of smooth basis functions for constructing approximate solution  $\hat{u} \in V_{M_u}$

$M$ : number of basis functions for calculating  $\lambda^M$

$\|F(\hat{u})\|_{H^{-1}}$ : upper bound for the residual norm estimated via (3.15)

$\|F'_{\hat{u}}{}^{-1}\|_{\mathcal{L}(H^{-1}, H_0^1)}$ : upper bound for the inverse operator norm estimated via Theorem 9

$L$ : upper bound for Lipschitz constant satisfying (3.14)

$\alpha$ : upper bound for  $\alpha$  required in Theorem 8

$\beta$ : upper bound for  $\beta$  required in Theorem 8

$r_A$ : upper bound for absolute error  $\|u - \hat{u}\|_{H_0^1}$

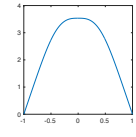
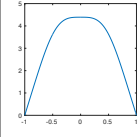
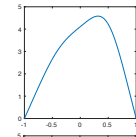
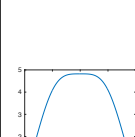
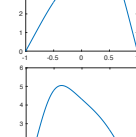
$r_R$ : upper bound for relative error  $\|u - \hat{u}\|_{H_0^1} / \|\hat{u}\|_{H_0^1}$

Next, we discuss how we have been able to verify solutions in areas not previously analyzed. We remark that S. Tanaka [30, 31] already proved that a symmetric solution and asymmetric solutions exist if  $l \geq 2$  with  $p = 3$ , and if  $l = 0$  then only one symmetric solution exists. Now, we focused in the interval  $0 < l \leq 2$  where previously unknown area.

Table 3.2 shows the approximate solutions together with their verification results where some sample points  $l = 1, 1.5, 1.75$ . To satisfy inequality (3.6), our program set  $\tau$  to the next floating-point number after a computed upper bound of the right side of (3.6). Therefore, when  $\hat{u}$  vanishes at some point on  $\bar{\Omega}$ ,  $\tau$  is set to the floating-point number after zero, which is approximately  $4.9407 \times 10^{-324}$ . In Table 3.2,  $\|F(\hat{u})\|_{H^{-1}}$ ,  $\|F'_{\hat{u}}\|_{\mathcal{L}(H^{-1}, H_0^1)}$ ,  $L$ ,  $\alpha$ , and  $\beta$  denote the constants required by Theorem 8. Moreover,  $r_A$  and  $r_R$  denote an upper bound for absolute error  $\|u - \hat{u}\|_{H_0^1}$  and relative error  $\|u - \hat{u}\|_{H_0^1} / \|\hat{u}\|_{H_0^1}$ , respectively. The values in row “Peak” represent upper bounds for the maximum values of the corresponding approximate solutions in decimal form.

The values in rows  $\mu_1 - \mu_5$  represent approximations of the five smallest eigenvalues of (3.18) discretized in  $V_M \subset H_0^1(\Omega)$ , which is spanned by the basis functions  $\phi_n$  ( $n = 1, 2, \dots, M$ ) without the restriction of symmetry. When  $l = 1$ , symmetric solutions have one negative eigenvalue. When  $l = 1.5, 1.75$ , symmetric solutions have two negative eigenvalues and asymmetric solutions have one negative eigenvalue.

Table 3.2 Verification results for  $p = 3, l = 1, 1.5, 1.75$ .

$l$	1	1.5		1.75	
$\hat{u}$					
$M_u$	60	70	70	40	40
$M$	40	40	40	40	40
$\ F(\hat{u})\ _{H^{-1}}$	9.61364e-5	1.33983e-5	3.93196e-4	4.74513e-5	8.24456e-4
$\ F'_{\hat{u}}\ _{\mathcal{L}(H^{-1}, H_0^1)}$	1.76503e+1	1.07965e+1	7.65807	5.94630	4.32131
$L$	1.51833e+1	1.92976e+1	1.87386e+1	2.14042e+1	2.02870e+1
$\alpha$	1.69684e-3	1.44654e-4	3.01112e-3	2.82160e-4	3.56273e-3
$\beta$	2.67988e+2	2.08346e+2	1.43501e+2	1.27276e+2	8.76663e+1
$r_A$	3.52331e-3	1.95542e-4	5.53575e-3	3.50669e-4	5.19979e-3
$r_R$	6.00061e-4	2.56602e-5	7.29735e-4	4.10380e-5	6.16444e-4
Peak	3.53591	4.39542	4.60383	4.82846	5.07378
$\mu_1$	-1.99999	-1.99999	-1.99999	-2.00000	-1.99999
$\mu_2$	0.076502	-0.09263	0.164225	-0.16818	0.272274
$\mu_3$	0.735955	0.717610	0.695956	0.710254	0.684876
$\mu_4$	0.825836	0.802359	0.855733	0.792345	0.865012
$\mu_5$	0.907874	0.900254	0.892713	0.897159	0.899653

$M_u$ : number of smooth basis functions for constructing approximate solution  $\hat{u} \in V_{M_u}$   
 $M$ : number of basis functions for calculating  $\lambda^M$   
 $\|F(\hat{u})\|_{H^{-1}}$ : upper bound for the residual norm estimated via (3.15)  
 $\|F'_{\hat{u}}\|_{\mathcal{L}(H^{-1}, H_0^1)}$ : upper bound for the inverse operator norm estimated via Theorem 9  
 $L$ : upper bound for Lipschitz constant satisfying (3.14)  
 $\alpha$ : upper bound for  $\alpha$  required in Theorem 8  
 $\beta$ : upper bound for  $\beta$  required in Theorem 8  
 $r_A$ : upper bound for absolute error  $\|u - \hat{u}\|_{H_0^1}$   
 $r_R$ : upper bound for relative error  $\|u - \hat{u}\|_{H_0^1} / \|\hat{u}\|_{H_0^1}$   
 Peak: upper bound for the maximum values of the corresponding approximation



$\mu_1 - \mu_5$ : approximations of the five smallest eigenvalues of (3.18)

### 3.7 Branches

In this section, we introduce the method of verifying solution branches of (3.2) based on [10, Section 9.1 Solution Branches]. Here, we are interested in the problem depending on a real parameter  $l$  (with a fixed parameter  $p$ ), and not only in solutions  $u$  for one or finitely many selected values of  $l$ , but in branches  $(u_l)_{l \in I}$  of solutions depending smoothly on the parameter  $l$  within some compact interval  $I \subset \mathbb{R}$ . Let  $J \subset \mathbb{R}$  be some open interval, and we extend (3.10) and consider the problem

$$F(u, l) = 0, \quad (3.29)$$

with the continuously Fréchet differentiable mapping  $F : H_0^1(\Omega) \times J \rightarrow H^{-1}$ . Let  $D_u F[v, l] : H_0^1(\Omega) \rightarrow H^{-1}$  be the Fréchet derivative in the  $u$ -direction at  $v \in H_0^1(\Omega)$ . Suppose that, for finitely many parameter values  $l_0, \dots, l_M \in J$ , ordered according to

$$l_0 < l_1 < \dots < l_M,$$

with “small” distances  $l_i - l_{i-1}$ , approximate solutions  $\hat{u}_0, \dots, \hat{u}_M \in H_0^1(\Omega)$  to problem (3.29) have been computed, giving rise to the conjecture that a continuum  $(u_l)_{l \in [l_0, l_M]}$  of solutions to problem (3.29), with  $u_{l_i}$  “close to”  $\hat{u}_i$ , exists.

We assume that, for each  $i \in \{0, \dots, M\}$ , constants  $\delta_i, K_i, L_i$  are known via the method presented in Sections 3.3 and 3.4 which satisfy

$$\|F(\hat{u}_i, l_i)\|_{H^{-1}} \leq \delta_i, \quad (3.30)$$

$$\left\| D_u F[\hat{u}_i, l_i]^{-1} \right\|_{\mathcal{L}(H^{-1}, H_0^1)} \leq K_i \quad (3.31)$$

$$\begin{aligned} \|D_u F[v, (1-t)l_{i-1} + tl_i] - D_u F[w, (1-t)l_{i-1} + tl_i]\|_{\mathcal{L}(H_0^1, H^{-1})} &\leq L_i \|v - w\|_{H_0^1}, \\ &\text{for all } v, w \in D \text{ and } t \in [0, 1], \end{aligned} \quad (3.32)$$

where,  $D = B((1-t)\hat{u}_{i-1} + t\hat{u}_i, \delta_i K_i + \delta_{i-1} K_{i-1} + \|\hat{u}_i - \hat{u}_{i-1}\|_{H_0^1}/2)$  is an open ball depending on the above value  $\delta_i > 0$  and  $K_i > 0$ . Now we define a  $l$ -piecewise linear (and  $l$ -continuous) approximate solution branch  $(\hat{u}^{(l)})_{l \in [l_0, l_M]}$  by

$$\hat{u}^{(l)} := \frac{l_i - l}{l_i - l_{i-1}} \hat{u}_{i-1} + \frac{l - l_{i-1}}{l_i - l_{i-1}} \hat{u}_i \quad (l_{i-1} \leq l \leq l_i, \quad i = 1, \dots, M) \quad (3.33)$$

Using these constants  $\delta_i, K_i, L_i$ , we have to compute piecewise constant and lower semi-continuous mappings  $[l_0, l_M] \rightarrow (0, M), l \mapsto \delta^{(l)}, l \mapsto K^{(l)}, l \mapsto L^{(l)}$ , such that

(a) The upper bound of the residual norm  $\delta^{(l)}$  satisfying

$$\|F(\hat{u}^{(l)}, l)\|_{H^{-1}} \leq \delta^{(l)}, \quad \text{for all } l \in [l_0, l_M], \quad (3.34)$$

(b) The upper bound of the inverse operator norm  $K^{(l)}$  satisfying

$$\left\| D_u F[\hat{u}^{(l)}, l]^{-1} \right\|_{\mathcal{L}(H^{-1}, H_0^1)} \leq K^{(l)}, \quad \text{for all } l \in [l_0, l_M], \quad (3.35)$$

(c) The upper bound of the Lipschitz constant  $L^{(l)}$  satisfying

$$\|D_u F[v, l] - D_u F[w, l]\|_{\mathcal{L}(H_0^1, H^{-1})} \leq L^{(l)} \|v - w\|_{H_0^1},$$

for all  $v, w \in D$  and  $l \in [l_0, l_M]$ ,

(3.36)

where,  $D = B(\hat{u}^{(l)}, 2\delta^{(l)}K^{(l)} + \delta)$  is an open ball depending on the above value  $\delta^{(l)} > 0$  and  $K^{(l)} > 0$  for small  $\delta > 0$ .

**ad (a)** We fix  $i \in \{0, \dots, M\}$  and  $l \in [l_{i-1}, l_i]$ , and define  $t := (l - l_{i-1}) / (l_i - l_{i-1}) \in [0, 1]$ , hence

$$l = (1 - t)l_{i-1} + tl_i, \quad \hat{u}^{(l)} = (1 - t)\hat{u}_{i-1} + t\hat{u}_i \quad (3.37)$$

Suppose that we know some  $\tau_i > 0$  (not depending on  $t$ ) such that

$$\|(1 - t)F(\hat{u}_{i-1}, l_{i-1}) + tF(\hat{u}_i, l_i) - F((1 - t)\hat{u}_{i-1} + t\hat{u}_i, (1 - t)l_{i-1} + tl_i)\|_{H^{-1}} \leq \tau_i \quad (3.38)$$

In our problem, the computation of  $\tau_i$  essentially reduces to computing some function  $\tilde{\tau}_i : \Omega \rightarrow [0, \infty)$  such that

$$|(1 - t)f(\hat{u}_{i-1}, l_{i-1}) + tf(\hat{u}_i, l_i) - f((1 - t)\hat{u}_{i-1} + t\hat{u}_i, (1 - t)l_{i-1} + tl_i)| \leq \tilde{\tau}_i(x) \quad (3.39)$$

for all  $x \in \Omega$  where we set  $f : H_0^1(\Omega) \times J \rightarrow H^{-1}$  as

$$f(u, l) := |x|^l u(x)^p.$$

Here  $f$  is twice continuously differentiable with respect to  $u$  and  $l$ , the standard interpolation error bound gives (3.39) for

$$\begin{aligned} \tilde{\tau}_i(x) := & \frac{1}{8} \left[ |\hat{u}_i(x) - \hat{u}_{i-1}(x)|^2 \max_{(y, \mu) \in A(x)} \left| \frac{\partial^2 f}{\partial y^2}(x, y, \mu) \right| \right. \\ & + 2 |\hat{u}_i(x) - \hat{u}_{i-1}(x)| |l_i - l_{i-1}| \max_{(y, \mu) \in A(x)} \left| \frac{\partial^2 f}{\partial y \partial l}(x, y, \mu) \right| \\ & \left. + |l_i - l_{i-1}|^2 \max_{(y, \mu) \in A(x)} \left| \frac{\partial^2 f}{\partial l^2}(x, y, \mu) \right| \right] \end{aligned} \quad (3.40)$$

where  $A(x) := [\min\{\hat{u}_{i-1}(x), \hat{u}_i(x)\}, \max\{\hat{u}_{i-1}(x), \hat{u}_i(x)\}] \times [l_{i-1}, l_i]$ .

Clearly,  $\tilde{\tau}_i(x)$  is quadratically small when  $l_i - l_{i-1}$  is sufficiently small, and the associated approximate solutions  $\hat{u}_i$  and  $\hat{u}_{i-1}$  are close to each other. It depends on choosing a sufficiently fine grid  $\{l_0, \dots, l_M\}$ .

Hence, also  $\tau_i$  satisfying (3.38) (computed based on  $\tilde{\tau}_i(x)$ ) will be quadratically small. By (3.37), (3.38), and the residual norm  $\|F(\hat{u}_i, l_i)\|_{H^{-1}}$ , it is now very simple to estimate

$$\begin{aligned} \|F(\hat{u}^{(l)}, l)\|_{H^{-1}} & \leq (1 - t)\|F(\hat{u}_{i-1}, l_{i-1})\|_{H^{-1}} + t\|F(\hat{u}_i, l_i)\|_{H^{-1}} + \tau_i \\ & \leq \max\{\delta_{i-1}, \delta_i\} + \tau_i \\ & =: \delta^{(l)}. \end{aligned}$$

Thus, the constant  $\delta^{(l)}$  is small when  $\delta_{i-1}$  and  $\delta_i$  are small (i.e. when  $\hat{u}_{i-1}$  and  $\hat{u}_i$  have been computed with sufficient accuracy) and the grid points  $l_{i-1}$  and  $l_i$  (and the associated approximate solutions  $\hat{u}_{i-1}$  and  $\hat{u}_i$ ) are sufficiently close to each other.

**ad (b),(c)** We fix  $i \in \{0, \dots, M\}$  and  $l \in [\frac{1}{2}(l_{i-1} + l_i), \frac{1}{2}(l_i + l_{i+1})]$ , where we formally put  $l_{-1} := l_0, l_{M+1} := l_M$ . Hereafter, we denote  $d_\mu(x) := |x|^{l_i}(|x|^\mu - 1)$ , and assume that some  $\rho_i > 0$  has been computed such that

$$\begin{aligned}
& \|D_u F[\hat{u}_i, l_i + \mu] - D_u F[\hat{u}_i, l_i]\|_{\mathcal{L}(H_0^1, H^{-1})} \\
& \leq p \sup_{0 \neq \phi \in H_0^1} \sup_{0 \neq \psi \in H_0^1} \frac{|\int_{\Omega} (|x|^{l_i + \mu} |\hat{u}_i(x)|^{p-1} \phi(x) - |x|^{l_i} |\hat{u}_i(x)|^{p-1} \phi(x)) \psi(x) dx|}{\|\phi\|_{H_0^1} \|\psi\|_{H_0^1}} \\
& = p \sup_{0 \neq \phi \in H_0^1} \sup_{0 \neq \psi \in H_0^1} \frac{|\int_{\Omega} d_\mu(x) |\hat{u}_i(x)|^{p-1} \phi(x) \psi(x) dx|}{\|\phi\|_{H_0^1} \|\psi\|_{H_0^1}} \\
& \leq p \sup_{0 \neq \phi \in H_0^1} \sup_{0 \neq \psi \in H_0^1} \frac{\|d_\mu \hat{u}_i^{p-1}\|_{L^{p+1}} \|\phi\|_{L^{p+1}} \|\psi\|_{L^{p+1}}}{\|\phi\|_{H_0^1} \|\psi\|_{H_0^1}} \\
& \leq p C_{p+1}^2 \|d_\mu \hat{u}_i^{p-1}\|_{L^{p+1}} =: \rho_i \quad \text{for all } \mu \in \left[-\frac{1}{2}(l_i - l_{i-1}), \frac{1}{2}(l_{i+1} - l_i)\right]. \quad (3.41)
\end{aligned}$$

Furthermore, we suppose that the grid  $\{l_0, \dots, l_M\}$  has been chosen fine enough, and that also the associated approximate solutions are sufficiently close to each other, to ensure that

$$\kappa_i := \max \left\{ L_i \left( \frac{1}{2} \|\hat{u}_i - \hat{u}_{i-1}\|_{H_0^1} \right), L_{i+1} \left( \frac{1}{2} \|\hat{u}_{i+1} - \hat{u}_i\|_{H_0^1} \right) \right\} + \rho_i < \frac{1}{K_i}, \quad (3.42)$$

with  $K_i$  from (3.31) and  $L_i$  from (3.32); here we formally have to put the  $L_0$ -term and the  $L_{M+1}$ -term occurring in (3.42) for  $i = 0$  and for  $i = M$ , respectively, equal to zero.

Now suppose first that  $i \geq 1$  and  $l \in [\frac{1}{2}(l_{i-1} + l_i), l_i]$ , and define  $t := (l - l_{i-1}) / (l_i - l_{i-1}) \in [\frac{1}{2}, 1]$ , whence again (3.37) holds. Therefore,

$$\begin{aligned}
& \left\| D_u F[\hat{u}^{(l)}, l] - D_u F[\hat{u}_i, l_i] \right\|_{\mathcal{L}(H_0^1, H^{-1})} \leq \\
& \|D_u F[(1-t)\hat{u}_{i-1} + t\hat{u}_i, (1-t)l_{i-1} + tl_i] - D_u F[\hat{u}_i, (1-t)l_{i-1} + tl_i]\|_{\mathcal{L}(H_0^1, H^{-1})} \\
& \quad + \|D_u F[\hat{u}_i, (1-t)l_{i-1} + tl_i] - D_u F[\hat{u}_i, l_i]\|_{\mathcal{L}(H_0^1, H^{-1})} \\
& \leq L_i \left( (1-t) \|\hat{u}_i - \hat{u}_{i-1}\|_{H_0^1} \right) + \rho_i \leq \kappa_i, \quad (3.43)
\end{aligned}$$

using (3.32) for  $u := (1-t)(\hat{u}_i - \hat{u}_{i-1})$ , and (3.41) for  $\mu := -(1-t)(l_i - l_{i-1})$  in the last line. (3.43) together with (3.31) and (3.42) implies that  $\|R_l\|_{\mathcal{L}(H_0^1, H^{-1})} < 1$  for  $R_l := D_u F[\hat{u}_i, l_i]^{-1} (D_u F[\hat{u}^{(l)}, l] - D_u F[\hat{u}_i, l_i])$ , and hence  $D_u F(\hat{u}^{(l)}, l) = D_u F(\hat{u}_i, l_i) (id_{H_0^1} + R_l)$  is bijective.

If  $i \leq M-1$  and  $l \in [l_i, \frac{1}{2}(l_i + l_{i+1})]$ , we define  $t := (l - l_i) / (l_{i+1} - l_i) \in [0, 1/2]$ , whence (3.37) holds with  $i$  replaced by  $i+1$ . A calculation similar to the one leading to (3.43) now gives

$$\left\| D_u F[\hat{u}^{(l)}, l] - D_u F[\hat{u}_i, l_i] \right\|_{\mathcal{L}(H_0^1, H^{-1})} \leq L_{i+1} \left( t \|\hat{u}_{i+1} - \hat{u}_i\|_{H_0^1} \right) + \rho_i \leq \kappa_i \quad (3.44)$$

and bijectivity of  $D_u F [\hat{u}^{(l)}, l]$  follows as before.

Using (3.31) and (3.43), (3.44), we obtain, for each  $u \in H_0^1$ ,

$$\|u\|_{H_0^1} \leq K_i \|D_u F [\hat{u}_i, l_i][u]\|_{H^{-1}} \leq K_i \left( \|D_u F [\hat{u}^{(l)}, l][u]\|_{H^{-1}} + \kappa_i \|u\|_{H_0^1} \right),$$

which by our assumption (3.42) implies that (3.35) holds, for  $l \in [\frac{1}{2}(l_{i-1} + l_i), \frac{1}{2}(l_i + l_{i+1})]$ , when we choose

$$K^{(l)} := \frac{K_i}{1 - K_i \kappa_i} \tag{3.45}$$

In this way we obtain a piecewise constant function  $[l_0, l_M] \rightarrow (0, \infty), l \mapsto K^{(l)}$ . Choosing again the smaller of the two values at the points  $\frac{1}{2}(l_{i-1} + l_i)$  ( $i = 1, \dots, M$ ), where  $K^{(l)}$  is possibly doubly defined by (3.45), this mapping is lower semi-continuous.

Finally we define the Lipschitz constant  $L^{(l)}$ , for  $l \in [l_{i-1}, l_i]$  ( $i = 1, \dots, M$ ),

$$L^{(l)} := L_i$$

and then, we can set  $\alpha^{(l)}$  and  $\beta^{(l)}$  such that

$$\begin{aligned} \alpha^{(l)} &= \delta^{(l)} K^{(l)}, \\ \beta^{(l)} &= K^{(l)} L^{(l)}. \end{aligned}$$

Here, if

$$\alpha^{(l)} \beta^{(l)} \leq \frac{1}{2}, \tag{3.46}$$

is satisfied we can verify the solution  $u^{(l)}$  based on Theorem 8. (3.46) for each  $l \in [l_0, l_M]$  amount to finitely many inequalities which are therefore computer-tractable.

### 3.8 Numerical results of bifurcation branches

In this section, we present numerical results of bifurcation branches for (3.2). Our approximate computation obtained Figure 3.1, the solution curves of (3.1) with  $p = 3$  for  $0 \leq l \leq 4$  ( $l$  is always a multiple of  $2^{-7}$ ). We remark that S. Tanaka already proved the existence of a symmetric solution and asymmetric solutions [30, 31] when  $l \geq 4$ , so we focused in the interval  $0 \leq l \leq 4$ . First, we computed approximate solutions  $\hat{u}_0, \dots, \hat{u}_M \in H_0^1(\Omega)$  with  $M_u = 40$ , as well as constants  $\delta_0, \dots, \delta_M$ , constants  $K_0, \dots, K_M$ , and constants  $L_0, \dots, L_M$  are satisfying Newton–Kantorovich theorem. Then, we applied the verification method of section 3.7 for symmetric solution’s lines (blue lines in Figure 3.1) and asymmetric solution’s lines (orange lines in Figure 3.1). As a result, symmetric solution’s lines where  $0 \leq l \leq 1$ ,  $1.5 \leq l \leq 4$ , and asymmetric solution’s lines where  $1.5 \leq l \leq 4$  are verified. Tables 3.3, 3.4 contains the computed values  $\delta^{(l)}$ ,  $K^{(l)}$ ,  $L^{(l)}$ ,  $\alpha^{(l)}$ ,  $\beta^{(l)}$  for some of the  $l$ -intervals.

The next goal is to find and verify the bifurcation point that corresponds to the red dot on Figure 3.1.

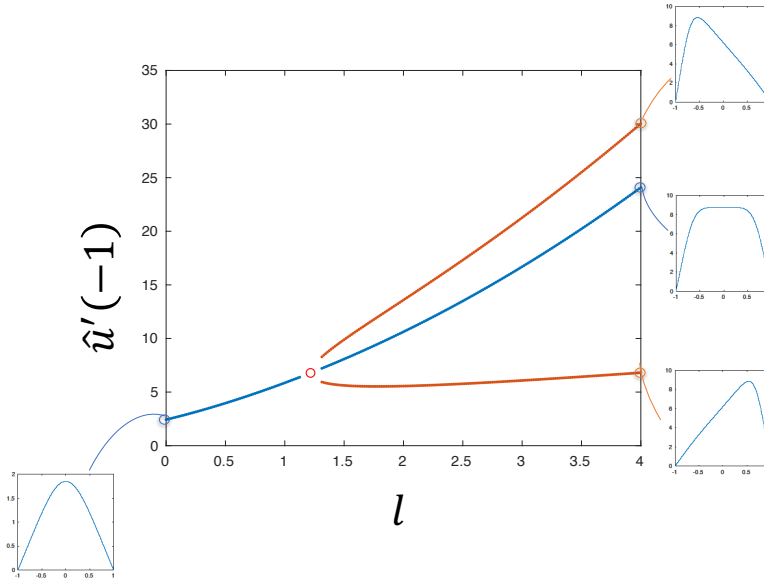
Figure 3.1 Solution curves for (3.2) with  $p = 3$ .

Table 3.3 Verification results for symmetric branch.

$l$ -interval	$\delta^{(l)}$	$K^{(l)}$	$L^{(l)}$	$\alpha^{(l)}$	$\beta^{(l)}$	$\alpha^{(l)}\beta^{(l)}$
$(0.5, 0.5 + 2^{-7})$	3.24322e-4	5.34505	11.2525	1.73352e-3	60.1450	0.10426
$(1, 1 + 2^{-10})$	3.99253e-5	22.2019	15.1826	8.86415e-4	3.37082e+2	0.29880
$(1.5, 1.5 + 2^{-10})$	1.34583e-5	12.7289	19.3053	1.71307e-4	2.45734e+2	4.20961e-2
$(3, 3 + 2^{-7})$	6.64243e-4	3.66165	32.2902	2.43223e-3	1.18236e+2	0.28758

Table 3.4 Verification results for asymmetric branch.

$l$ -interval	$\delta^{(l)}$	$K^{(l)}$	$L^{(l)}$	$\alpha^{(l)}$	$\beta^{(l)}$	$\alpha^{(l)}\beta^{(l)}$
$(1.5, 1.5 + 2^{-10})$	2.69964e-4	8.44707	18.7367	2.28041e-3	1.58270e+2	0.36092
$(3, 3 + 2^{-7})$	2.81497e-4	2.96478	27.9466	8.34578e-4	82.8556	6.91494e-2

### 3.9 Bifurcation point

This section discusses the numerical verification method to find the symmetry breaking bifurcation point of the problem (3.2) for the parameter  $l$ . We consider an expanded equation that resolves the singularity that arises at the bifurcation point.

Let  $V_s$  be a symmetric subspace of  $H_0^1(\Omega)$  and the topological dual space of  $V_s$  is denoted by  $V_s^*$ . Let  $A_s : V_s \rightarrow V_s^*$  as

$$\langle A_s u, v \rangle = (u, v)_{V_s}, u, v \in V_s,$$

and  $f : V_s \times \mathbb{R} \rightarrow V_s^*$  as

$$f(u, l) := |x|^l u(x)^p,$$

and  $F_1 : V_s \times \mathbb{R} \rightarrow V_s^*$  as

$$F_1(u, l) := A_s u - f(u, l).$$

Then, the one-dimensional Hénon equation (3.2) can be described as

$$F_1(u, l) = 0.$$

Moreover, let  $F_1$  be Fréchet differentiable in the  $u$ -direction, and let  $D_u F_1[v, l] : V_s \rightarrow V_s^*$  be the Fréchet derivative in the  $u$ -direction at  $v \in H_0^1(\Omega)$ . Next, let  $V_a$  be an asymmetric subspace of  $H_0^1(\Omega)$  and we set the solution space  $\mathbf{V} = V_s \times V_a \times \mathbb{R}$ . The solution space  $\mathbf{V}$  is a Hilbert space because it consists of a direct product of Hilbert spaces. Then, the symmetry breaking bifurcation point is  $l$  satisfying the problem

$$\text{Find } (u, \phi, l) \in \mathbf{V} \text{ s.t. } \begin{pmatrix} F_1(u, l) \\ D_u F_1[u, l]\phi \\ \|\phi\|_{L^2}^2 - 1 \end{pmatrix} = \begin{pmatrix} 0 \\ 0 \\ 0 \end{pmatrix}.$$

In other words, let  $F_1, F_2, F_3$  be

$$\begin{aligned} F_1(u, l) &:= A_s u - |x|^l u^p && : V_s \times \mathbb{R} \rightarrow V_s^*, \\ F_2(u, \phi, l) &:= A_a \phi - p|x|^l u^{p-1} \phi && : V_s \times V_a \times \mathbb{R} \rightarrow V_a^*, \\ F_3(\phi) &:= \|\phi\|_{L^2}^2 - 1 && : V_a \rightarrow \mathbb{R}, \end{aligned}$$

and  $F : \mathbf{V} \rightarrow \mathbf{V}^*$  be

$$F(u, \phi, l) := \begin{pmatrix} F_1(u, l) \\ F_2(u, \phi, l) \\ F_3(\phi) \end{pmatrix}$$

where  $\mathbf{V}^* = V_s^* \times V_a^* \times \mathbb{R}$ . Then we define  $\mathbf{u} := (u, \phi, l)$  and we consider the following problem

$$\text{Find } \mathbf{u} \in \mathbf{V} \text{ s.t. } F(\mathbf{u}) = \mathbf{0}. \quad (3.47)$$

To conduct the numerical verification for this problem, we also apply the Newton–Kantorovich theorem (Theorem 8), which enables us to prove the existence of a true solution  $\mathbf{u}$  in  $\bar{B}(\hat{\mathbf{u}}, \rho)$ . Then, we can prove that the bifurcation point  $l$  exists in  $\bar{B}(\hat{l}, \rho)$ . We are left to evaluate the residual norm  $\|F(\hat{\mathbf{u}})\|_{\mathbf{V}^*}$ , the inverse operator norm  $\|F'_{\hat{\mathbf{u}}}\|_{\mathcal{L}(\mathbf{V}^*, \mathbf{V})}$ , and the Lipschitz constant  $L$  for problem (3.47).

The residual norm  $\|F(\hat{\mathbf{u}})\|_{\mathbf{V}^*}$  can be evaluated as follows

$$\|F(\hat{\mathbf{u}})\|_{\mathbf{V}^*} \leq \sqrt{\|F_1(\hat{\mathbf{u}})\|_{V_s^*}^2 + \|F_2(\hat{\mathbf{u}})\|_{V_a^*}^2 + \|F_3(\hat{\mathbf{u}})\|_{\mathbb{R}}^2}.$$

For the problem (3.47), the inverse operator norm  $\|F'_{\hat{\mathbf{u}}}\|_{\mathcal{L}(\mathbf{V}^*, \mathbf{V})}$  cannot be evaluated in the way that is based on Theorem 9. In such cases, there is a method by Nakao et al [10, Theorem 3.17]. First, we set operators  $\mathcal{A} : \mathbf{V} \rightarrow \mathbf{V}^*$  and  $f : \mathbf{V} \rightarrow \mathbf{V}^*$  are defined by

$$\mathcal{A} := \begin{pmatrix} A_s & 0 & 0 \\ 0 & A_a & 0 \\ 0 & 0 & 1 \end{pmatrix},$$

and

$$f(\mathbf{u}) := \begin{pmatrix} |x|^l u^p \\ p|x|^l u^{p-1} \phi \\ \|\phi\|_{L^2}^2 - 1 \end{pmatrix},$$

For  $\mathbf{u} \in \mathbf{V}$ , the Ritz projection  $R_h : \mathbf{V} \rightarrow \mathbf{V}_h$  is defined by

$$((I - R_h)\mathbf{u}, \mathbf{v}_h)_{\mathbf{V}} = 0, \mathbf{v}_h \in \mathbf{V}_h,$$

where  $\mathbf{V}_h$  is a finite-dimensional subspace of  $\mathbf{V}$ . Let  $\mathbf{V}_{\perp} := \{\mathbf{u} \in \mathbf{V} : (\mathbf{u}, \mathbf{v}_h)_{\mathbf{V}} = 0, \mathbf{v}_h \in \mathbf{V}_h\}$  be an orthogonal complement of  $\mathbf{V}_h$ . Let  $f'_v : \mathbf{V} \rightarrow \mathbf{V}_h$  be the Fréchet derivative at  $\mathbf{v} \in \mathbf{V}$  of nonlinear term  $f(\mathbf{u})$ , and  $F'_v$  be a linear operator defined by

$$F'_v := \mathcal{A} - f'_v.$$

Let  $T : \mathbf{V}_h \rightarrow \mathbf{V}_h$  be a finite-dimensional operator:

$$T = R_h \mathcal{A}^{-1} F'_{\hat{\mathbf{u}}} |_{\mathbf{V}_h}$$

where  $\cdot |_{\mathcal{X}}$  denotes the restriction for the domain of the operator. Let  $B : \mathbf{V}_{\perp} \rightarrow \mathbf{V}_{\perp}$  be a linear operator defined by

$$B := (I - R_h) \mathcal{A}^{-1} f'_{\hat{\mathbf{u}}} |_{\mathbf{V}_{\perp}} + (I - R_h) \mathcal{A}^{-1} f'_{\hat{\mathbf{u}}} |_{\mathbf{V}_h} T^{-1} R_h \mathcal{A}^{-1} f'_{\hat{\mathbf{u}}} |_{\mathbf{V}_{\perp}}.$$

Let  $S : \mathbf{V}_{\perp} \rightarrow \mathbf{V}_{\perp}$  be a linear operator defined by

$$S := I_{\mathbf{V}_{\perp}} - B$$

Then, following theorem can be used.

**Theorem 12** [33, Corollary 1] *It follows that*

$$\|F'_{\hat{\mathbf{u}}}^{-1}\|_{\mathcal{L}(\mathbf{V}^*, \mathbf{V})} \leq \left\| \begin{pmatrix} \left\| T^{-1} + T^{-1} \mathcal{A}_h^{-1} f'_{\hat{\mathbf{u}}} |_{\mathbf{V}_{\perp}} S^{-1} \mathcal{A}_{\perp}^{-1} f'_{\hat{\mathbf{u}}} |_{\mathbf{V}_h} T^{-1} \right\|_{\mathcal{L}(\mathbf{V}, \mathbf{V})} & \left\| T^{-1} \mathcal{A}_h^{-1} f'_{\hat{\mathbf{u}}} |_{\mathbf{V}_{\perp}} S^{-1} \right\|_{\mathcal{L}(\mathbf{V}, \mathbf{V})} \\ \left\| S^{-1} \mathcal{A}_{\perp}^{-1} f'_{\hat{\mathbf{u}}} |_{\mathbf{V}_h} T^{-1} \right\|_{\mathcal{L}(\mathbf{V}, \mathbf{V})} & \left\| S^{-1} \right\|_{\mathcal{L}(\mathbf{V}, \mathbf{V})} \end{pmatrix} \right\|_E,$$

where  $\|\cdot\|_E$  denotes a matrix norm induced by the Euclidean vector norm  $|\cdot|_E$ .

Subsequently, the Lipschitz constant  $L$  can be evaluated as follows :

$$L \leq \left\| \int_0^1 F''_{\hat{\mathbf{u}}+2\alpha t} dt \right\|_{\mathcal{L}(\mathbf{V}, \mathbf{V})}.$$

by applying [34, Corollary 1]. Then, we set  $\alpha$  and  $\beta$  such that

$$\begin{aligned} \alpha &= \|F(\hat{\mathbf{u}})\|_{\mathbf{V}^*} \|F'_{\hat{\mathbf{u}}}^{-1}\|_{\mathcal{L}(\mathbf{V}^*, \mathbf{V})}, \\ \beta &= \|F'_{\hat{\mathbf{u}}}^{-1}\|_{\mathcal{L}(\mathbf{V}^*, \mathbf{V})} L, \end{aligned}$$

and if

$$\alpha\beta \leq \frac{1}{2}, \tag{3.48}$$

then there exists a solution  $\mathbf{u} \in \mathbf{V}$  of  $F(\mathbf{u}) = 0$  in  $\bar{B}(\hat{\mathbf{u}}, \rho)$  with

$$\rho = \frac{1 - \sqrt{1 - 2\alpha\beta}}{\beta},$$

based on Theorem 8. Finally, there exists a true bifurcation point  $l \in \mathbb{R}$  in  $\bar{B}(\hat{l}, \rho)$ , because

$$|l - \hat{l}| \leq \|\mathbf{u} - \hat{\mathbf{u}}\|_{\mathbf{V}}.$$

In other words, there exists a true bifurcation point  $l$  in the interval  $[\hat{l} - \rho, \hat{l} + \rho]$ .

**Remark 2** “log type singularity” and improvement of *fpsa* and *vfpsa*

When generating Jacobi matrices of (3.47), we need to integrate over the form  $|x|^l \log|x|u^p$  by partial differentiation of parameter  $l$  for the terms in  $|x|^l u^p$ . We added a element for the integration of *fpsa* and *vfpsa*. In order to deal with the “algebraic type singularity” and the “log type singularity”, the following integration is performed.

- Integration (“algebraic type singularity” + “log type singularity”):

$$\begin{aligned} & \int_{-1}^1 |x|^a \log|x| \mathcal{P}(x) dx \\ &= \int_{-1}^1 |x|^a \log|x| (t_0 + t_1 x + \dots + t_n x^n) dx \\ &= \int_0^1 x^a \log x (t_0 + t_1 x + \dots + t_n x^n) dx + \int_{-1}^0 (-x)^a \log(-x) (t_0 + t_1 x + \dots + t_n x^n) dx \\ &= \int_0^1 (t_0 x^a \log x + t_1 x^{1+a} \log x + \dots + t_n x^{n+a} \log x) dx \\ & \quad + \int_0^1 (t_0 y^a \log y - t_1 y^{1+a} \log y + \dots + t_n y^{n+a} \log y) dy \\ &= \left[ t_0 \frac{(1+a) \log x - 1}{(1+a)^2} x^{1+a} + t_1 \frac{(2+a) \log x - 1}{(2+a)^2} x^{2+a} + \dots + t_n \frac{(n+1+a) \log x - 1}{(n+1+a)^2} x^{n+1+a} \right]_0^1 \\ & \quad + \left[ t_0 \frac{(1+a) \log y - 1}{(1+a)^2} y^{1+a} - t_1 \frac{(2+a) \log y - 1}{(2+a)^2} y^{2+a} + \dots + t_n \frac{(n+1+a) \log y - 1}{(n+1+a)^2} y^{n+1+a} \right]_0^1 \end{aligned}$$

### 3.10 Numerical results of the bifurcation point

In this section, we present numerical results of the bifurcation point for (3.2) with  $p = 3$  like the red dot on Figure 3.1. First, we computed approximate solutions  $\hat{\mathbf{u}} = (\hat{u}, \hat{\phi}, \hat{l})$  with  $M_u = 100$  (see Table 3.5). Next, we computed the residual norm  $\|F(\hat{\mathbf{u}})\|_{\mathbf{V}^*}$ , the inverse operator norm  $\|F'_{\hat{\mathbf{u}}}{}^{-1}\|_{\mathcal{L}(\mathbf{V}^*, \mathbf{V})}$ , and the Lipschitz constant  $L$  based on the section 3.9 to apply the Newton–Kantorovich theorem. As a result, we got the approximate bifurcation point

$$\hat{l} = 1.216895863752014$$



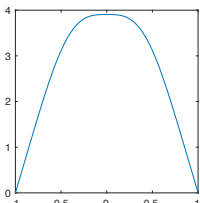
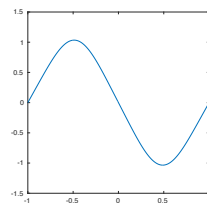
and the error upper bound is

$$\rho = 6.227185573261e - 4.$$

Therefore, the exact bifurcation point  $l$  exists in the interval

$$l \in [1.21627314519468, 1.21751858230934].$$

Table 3.5 Approximate solution  $\hat{u}$  at the bifurcation point ( $p = 3$ ).

$\hat{u}$	$\hat{\phi}$	$\hat{l}$
		1.216895863752014

### 3.11 Short summary of chapter 3

We designed a numerical verification method for proving the existence of solutions of the one-dimensional Hénon equation (3.2) on a bounded domain based on the Newton-Kantorovich theorem. We applied our method that follows the singularity of the Hénon equation, proving the existence of several solutions of (3.2) nearby a numerically computed approximation  $\hat{u}$  efficiently. As a result, we succeeded in verifying the branches and bifurcation points of the simple symmetry-breaking bifurcation in Figure 3.1.

## Chapter 4

# Conclusion

In chapter 2, we designed a numerical verification method for proving the existence of solutions of the Hénon equation (2.1) on a bounded domain based on the Newton-Kantorovich theorem. We applied our method to the domains  $\Omega = (0, 1)^N$  ( $N = 1, 2$ ), proving the existence of several solutions of (2.1) nearby a numerically computed approximation  $\hat{u}$ . In particular, we found a set of undiscovered solutions with three peaks on the square domain  $\Omega = (0, 1)^2$ . Approximate computations generated the solution curves of (2.1) for  $0 \leq l \leq 8$  in Figures 2.1 and 2.2.

In chapter 3, we designed a numerical verification method for proving the existence of solutions of the one-dimensional Hénon equation (3.2) on a bounded domain based on the Newton-Kantorovich theorem. We applied our method that follows the singularity of the Hénon equation, proving the existence of several solutions of (3.2) nearby a numerically computed approximation  $\hat{u}$  efficiently. As a result, we succeeded in verifying the branches and bifurcation points of the simple symmetry-breaking bifurcation in Figure 3.1.

In future work, we would like to deal with the Hénon equation (2.1) extended to high-dimensional domains  $\Omega$ . We aim to achieve this goal by implementing fast numerical integration of multivariate functions with singularity. Eventually, we would like to reveal all solution types in various domains through an algorithm for enclosing all solutions.

# Acknowledgments

I thank Dr. Kazuaki Tanaka (Waseda University, Japan), Dr. Kouta Sekine (Chiba Institute of Technology, Japan), and Prof. Shin'ichi Oishi (Waseda University, Japan) for their helpful advice. Prof. Kazunaga Tanaka (Waseda University, Japan), Prof. Kousuke Kuto (Waseda University, Japan), and Prof. Masahide Kashiwagi (Waseda University, Japan) were the sub-chief examiners of my doctoral thesis. I also express my gratitude to the sub-chief examiners for their insightful comments.

Taisei Asai  
December 2022

## References

- [1] M. Hénon, Numerical experiments on the stability of spherical stellar systems, *Astronomy and astrophysics* 24 (1973) 229–238.
- [2] B. Gidas, W.-M. Ni, L. Nirenberg, Symmetry and related properties via the maximum principle, *Communications in Mathematical Physics* 68 (3) (1979) 209–243.
- [3] B. Breuer, M. Plum, P. McKenna, Inclusions and existence proofs for solutions of a nonlinear boundary value problem by spectral numerical methods, in: *Topics in Numerical Analysis*, Springer 15, (2001) 61–77.
- [4] D. Smets, M. Willem, J. Su, Non-radial ground states for the Hénon equation, *Communications in Contemporary Mathematics* 4 (03) (2002) 467–480.
- [5] A. L. Amadori, F. Gladiali, Bifurcation and symmetry breaking for the Hénon equation, *Advances in Differential Equations* 19 (7/8) (2014) 755–782.
- [6] Z. Yang, Z. Li, H. Zhu, Bifurcation method for solving multiple positive solutions to Henon equation, *Science in China Series A: Mathematics* 51 (12) (2008) 2330–2342.
- [7] Z. Li, Z. Yang, H. Zhu, Bifurcation method for computing the multiple positive solutions to p-Henon equation, *Applied Mathematics and Computation* 220 (2013) 593–601.
- [8] Z. Li, Z. Yang, H. Zhu, A bifurcation method for solving multiple positive solutions to the boundary value problem of the Henon equation on a unit disk, *Computers & Mathematics with Applications* 62 (10) (2011) 3775–3784.
- [9] Z. Li, H. Zhu, Z. Yang, Bifurcation method for solving multiple positive solutions to Henon equation on the unit cube, *Communications in Nonlinear Science and Numerical Simulation* 16 (9) (2011) 3673–3683.
- [10] M. T. Nakao, M. Plum, Y. Watanabe, *Numerical Verification Methods and Computer-Assisted Proofs for Partial Differential Equations*, Springer, (2019).
- [11] K. Tanaka, K. Sekine, M. Mizuguchi, S. Oishi, Sharp numerical inclusion of the best constant for embedding  $H_0^1(\Omega) \hookrightarrow L^p(\Omega)$  on bounded convex domain, *Journal of Computational and Applied Mathematics* 311 (2017) 306–313.
- [12] P. Deuffhard, G. Heindl, Affine invariant convergence theorems for Newton’s method and extensions to related methods, *SIAM Journal on Numerical Analysis* 16 (1) (1979) 1–10.
- [13] M. Plum, Computer-assisted proofs for semilinear elliptic boundary value problems, *Japan journal of industrial and applied mathematics* 26 (2-3) (2009) 419–442.

- 
- [14] H. Behnke, The calculation of guaranteed bounds for eigenvalues using complementary variational principles, *Computing* 47 (1) (1991) 11–27.
- [15] S. M. Rump, Intlab–interval laboratory, in: *Developments in reliable computing*, Springer, (1999) 77–104.  
URL <http://www.ti3.tuhh.de/rump/>
- [16] S. Miyajima, Numerical enclosure for each eigenvalue in generalized eigenvalue problem, *Journal of Computational and Applied Mathematics* 236 (9) (2012) 2545–2552.
- [17] P. Grisvard, *Elliptic problems in nonsmooth domains*, SIAM, (2011).
- [18] K. Tanaka, A. Takayasu, X. Liu, S. Oishi, Verified norm estimation for the inverse of linear elliptic operators using eigenvalue evaluation, *Japan Journal of Industrial and Applied Mathematics* 31 (3) (2014) 665–679.
- [19] X. Liu, A framework of verified eigenvalue bounds for self-adjoint differential operators, *Applied Mathematics and Computation* 267 (2015) 341–355.
- [20] K. Tanaka, K. Sekine, S. Oishi, Numerical verification method for positivity of solutions to elliptic equations, *RIMS Kôkyûroku* 2037 (2011) 125–140.
- [21] S. Kimura, N. Yamamoto, On explicit bounds in the error for the  $H_0^1$ -projection into piecewise polynomial spaces, *Bulletin informatics and cybernetics* 31 (2) (1999) 109–115.
- [22] M. Kashiwagi, kv library, (2020).  
URL <http://verifiedby.me/kv/>
- [23] W. M. Ni, On the elliptic equation  $\Delta u + K(x)u^{(n+2)/(n-2)} = 0$ , its generalizations, and applications in geometry, *Indiana University Mathematics Journal* 31(4) (1982) 493–529.
- [24] W. M. Ni, S. Yotsutani, On Matukuma’s equation and related topics, *Proceedings of the Japan Academy, Series A, Mathematical Sciences* 62(7) (1986) 260–263.
- [25] K. Nagasaki, Radial solutions for on the unit ball in  $R^n$ , *Journal of the Faculty of Science, the University of Tokyo. Section 1A. Mathematics* 36(2) (1989) 211–232.
- [26] G. Chen, J. Zhou, W. M. Ni, Algorithms and visualization for solutions of nonlinear elliptic equations, *International Journal of Bifurcation and Chaos* 10(7) (2000) 1565–1612.
- [27] S. Didier, M. Willem, J. Su, Non-radial ground states for the Hénon equation, *Communications in Contemporary Mathematics* 4(3) (2002) 467–480.
- [28] J. Byeon, Z. Q. Wang, On the Hénon equation: asymptotic profile of ground states, I, *Annales de l’Institut Henri Poincaré C* 23(6) (2006) 803–828.
- [29] J. Byeon, Z. Q. Wang, On the Hénon equation: asymptotic profile of ground states, II, *Journal of Differential Equations*, 216(1) (2005) 78–108.
- [30] S. Tanaka, Morse index and symmetry-breaking for positive solutions of one-dimensional Hénon type equations, *Journal of Differential Equations* 255(7) (2013) 1709–1733.
- [31] I. Sim, S. Tanaka, Symmetry-breaking bifurcation for the one-dimensional Hénon equation, *Communications in Contemporary Mathematics* 21(1) (2019) 1–24.

- 
- [32] K. Kobayashi. A constructive a priori error estimation for finite element discretizations in a non-convex domain using singular functions. *Japan journal of industrial and applied mathematics* 26 (2) (2009) 493–516.
  - [33] K. Sekine, M. T. Nakao, S. Oishi, A new formulation using the Schur complement for the numerical existence proof of solutions to elliptic problems: without direct estimation for an inverse of the linearized operator, *Numer. Math.*, 146, (2020) 907–926.
  - [34] K. Sekine, M. T. Nakao, S. Oishi, Numerical verification methods for a system of elliptic PDEs, and their software library, *Nonlinear Theory and Its Applications, IEICE* 12.1 (2021): 41–74.

## List of research achievements for application of Doctor of Engineering, Waseda University

Full Name : 浅井 大晴

seal or signature

Date Submitted(yyyy/mm/dd): 2022/11/16

種類別 (By Type)	題名、発表・発行掲載誌名、 (theme, journal name, date & year of publication, name of authors inc. yourself)
論文(2件)	<p><b>O</b><u>Taisei Asai</u>, Kazuaki Tanaka, Shin'ichi Oishi: Numerical verification for asymmetric solutions of the Hénon equation on bounded domains, Journal of Computational and Applied Mathematics, 399, 113708 (2022). Journal (Open Access)</p>
国際学会発表 (6件)	<p>Kazuaki Tanaka, <b>Taisei Asai</b>: A posteriori verification of the positivity of solutions to elliptic boundary value problems, Partial Differential Equations and Application, 3, 9 (2022). Journal (Open Access)</p> <p>Kazuaki Tanaka, Kohei Yatabe, <b>Taisei Asai</b>, Sora Sawai: Rigorous simulation of reaction-diffusion models with neural networks, The 41st JSST Annual International Conference on Simulation Technology (JSST 2022), Online, Aug. 31, 2022. (査読有)</p> <p><b>Taisei Asai</b>, Kazuaki Tanaka, Kouta Sekine and Shin'ichi Oishi: Computer-assisted analysis for the bifurcation phenomena of the one-dimensional Henon-type equation, International Workshop on Reliable Computing and Computer-Assisted Proofs (ReCAP 2022), March 16, 2022.</p> <p><b>Taisei Asai</b>, Kazuaki Tanaka, Kouta Sekine and Shin'ichi Oishi: Computer-assisted analysis for bifurcation diagrams of the one-dimensional Henon equation, The 19th International Symposium on Scientific Computing, Computer Arithmetic, and Verified Numerical Computations (SCAN2020), September 14, 2021. (査読有)</p> <p><b>Taisei Asai</b>, Kazuaki Tanaka, and Shin'ichi Oishi: Numerical verification for positive solutions of the Hénon equation on some bounded domain, The 40th JSST Annual International Conference on Simulation Technology, September 2, 2021. (査読有)</p> <p><b>Taisei Asai</b>, Kazuaki Tanaka, and Shin'ichi Oishi: Existence proofs for asymmetric solutions of Hénon equation using verified numerical computations, International Workshop on the Verified Numerical Computations and its Applications (INVA), March 6-12, 2020 (conference cancelled).</p> <p><b>Taisei Asai</b>, Kazuaki Tanaka, and Shin'ichi Oishi: Numerical verification for asymmetric solutions of the Henon equation, The 38th JSST Annual International Conference on Simulation Technology, November 5th, 2019. (査読有)</p>
国内学会発表 (13件)	<p>多田秀介, <b>浅井大晴</b>, 田中一成, 大石進一: Batt-Faltenbacher-Horst 方程式の解の精度保証付き数値計算, 日本応用数理学会2022年度年会, Zoom, 2022年9月10日.</p> <p>松江要, 落合啓之, 小谷久寿, 佐々木多希子, <b>浅井大晴</b>: 常微分方程式の爆発解の複数項漸近展開, 日本数学会2022年度年会, 埼玉大学, 2022年3月30日.</p> <p>宮内洋明, 高安亮紀, 柏木雅英, <b>浅井大晴</b>: ベッセル関数のType-II PSAの計算について, 第18回(2021年度)日本応用数理学会研究部会連合発表会, Zoom, 2022年3月8日.</p>

## List of research achievements for application of Doctor of Engineering, Waseda University

Full Name : 浅井 大晴

seal or signature

Date Submitted(yyyy/mm/dd): 2022/11/16

種別 (By Type)	題名、発表・発行掲載誌名、 発表・発行年月、連名者（申請者含む） (theme, journal name, date & year of publication, name of authors inc. yourself)
	<p>松江要, 落合啓之, 小谷久寿, 佐々木多希子, <b>浅井大晴</b>: 常微分方程式の爆発解の複数項漸近展開, 2021年度応用数学合同研究集会, Zoom, 2021年12月17日.</p> <p><b>浅井大晴</b>, 田中一成, 関根晃太, 大石進一: 精度保証付き数値計算を用いた1次元エノン方程式の分岐図の解析, 第5回 精度保証付き数値計算の実問題への応用研究集会 (NVR 2021) (※ JST/CREST「モデリングのための精度保証付き数値計算論の展開」成果報告会と同時開催), 2021年11月28日 (Invited).</p> <p><b>浅井大晴</b>, 田中一成, 関根晃太, 大石進一: 精度保証付き数値計算を用いた1次元エノン型方程式に対する分岐解析, RIMS共同研究 (公開型) 「常微分方程式の定性的理論とその応用」, Zoom, 2021年11月11日 (Invited).</p> <p><b>浅井大晴</b>, 田中一成, 大石進一: 1次元エノン方程式の分岐図に対する計算機援用解析, 日本応用数学会2021年度年会, Zoom, 2021年9月9日.</p> <p><b>浅井大晴</b>, 田中一成, 大石進一: 特異関数を用いた1次元エノン方程式の解の精度保証付き数値計算, 応用数学会2021年研究部会連合発表会, 2021年3月4日.</p> <p><b>浅井大晴</b>, 田中一成, 大石進一: 精度保証付き数値計算を用いたHénon方程式の対称性に関する考察, 精度保証付き数値計算の実問題への応用研究集会 (NVR 2020), 2020年11月29日 (Invited).</p> <p><b>浅井大晴</b>, 田中一成, 大石進一: 精度保証付き数値計算を用いたHenon方程式の多重解の存在証明, 日本応用数学会2020年度年会, Zoom, 2020年9月10日.</p> <p>田中一成, <b>浅井大晴</b>: 楕円型境界値問題に対する解符号の事後検証法, 日本応用数学会2020年度年会, Zoom, 2020年9月10日.</p> <p><b>浅井大晴</b>, 田中一成, 大石進一: 精度保証付き数値計算を用いた Henon 方程式の非対称解の存在証明, 2019年度応用数学合同研究集会, 龍谷大学瀬田キャンパス, 2019年12月13日.</p> <p><b>浅井大晴</b>, 田中一成, 大石進一: Henon方程式の非対称解に対する精度保証付き数値計算, 日本応用数学会2019年度年会, 東京大学駒場キャンパス, 2019年9月3日～5日.</p>